Supplement of Atmos. Meas. Tech., 15, 6309–6328, 2022
https://doi.org/10.5194/amt-15-6309-2022-supplement


Atmospheric Measurement Techniques
Open Access

*Supplement of*

# Calibrating networks of low-cost air quality sensors

**Priyanka deSouza et al.**

*Correspondence to:* Priyanka deSouza (priyanka.desouza@ucdenver.edu)

# S1: Description of Machine Learning Algorithms Used For Calibration

1. *Random forest (RF)*: RF is a decision-tree-based machine learning algorithm that has been shown to perform well in air quality predictions. Briefly, to generate a random forest model, the user specifies the maximum number of trees that make up the forest. Each tree is constructed using a bootstrapped random sample from the training data set. The origin node of the decision tree is split into sub-nodes by considering a random subset of the possible explanatory variables. Trees are split based on which of the explanatory variables in each subset is the strongest predictor of the outcome. This process of node splitting is repeated until a terminal node is reached (Zimmerman et al., 2018). For our random forest models, the terminal node was specified using a minimum node size of five data points per node.

2. *Neural Network (NN)*: NN consists of interconnected neurons organized in layers. Each neuron or unit passes received information through an activation function and produces output values that are then processed by neurons in the next layer. The NN training process is based on updating the weights of neurons via supervised learning (Spinelle et al., 2014). A simple single hidden layer neural network with a linear transfer function was chosen in this study.

3. *Gradient Boosting (GB)*: GB is a decision-tree-based approach that uses ‘boosting’ methods to improve model performance. ‘Boosting’ sequentially combines many ‘weak’ models (learners) into a final, improved model. The final model is built in an additive forward stagewise manner where at each step a new learner is added that minimizes the negative gradient using a least squares approach. The residuals of the current model are then used as the input for the next tree allowing the model to ’learn' from the errors of the previous models (Johnson et al., 2018).

4. *SuperLearner (SL)*: SL is an ensemble-based machine learning algorithm, which allows for the simultaneous evaluation (by cross-validation) of a library of plausible machine learning algorithms to determine which models are most appropriate for the data, based on minimizing a least squares loss function, and then averages over these chosen models to produce a composite model (Van der Laan et al., 2007).

# S2 Cross-Validation techniques to avoid overfitting in the machine learning models

We used a Leave-One-Site (I25 Globeville, I25 Denver, La Casa, CAMP)-Out (LOSO) approach for cross validation (CV) to prevent overfitting in our machine learning models (Models 17 - 21 in **Table 2**). Briefly, we split the data into four groups, with each group excluding data from a single reference monitoring site. In each cross-validation iteration, we selected each group in turn to fit the model and made predictions at the left-out site. The model that had the best average performance across all the left out sites was chosen. In this manner this CV approach was used to tune the hyper parameters in the machine learning models adopted in this study using correction approaches: C1, C2, C3 and C4.

For the correction conducted on the complete archived dataset (C1), we also conducted a leave-out-by-date (LOBD) CV for the machine learning models considered (**Table 3**). For the LOBD model validation method, the project time period was split into 3-week periods. Each period contained between ~ 700 and 900 hourly data points, with typically more sensors running continuously during later chunks as more sensors were deployed and came online over time. Thirteen periods were available in total, and, for each test-train set, 12 periods were used to train the correction model, whereas the remaining interval was selected to test the correction model. The model that had the best average performance across all the left out time periods was chosen. By eliminating, using data from the same calendar week, where measurements are likely to be correlated, we eliminate the possibility of obtaining overly optimistic model performance summary statistics.

Zusman et al., (2020) have reported that for more than 3 co-location sites, a LOSO CV is preferred, as it replicates our ultimate objective of applying the calibration developed to other sites in the network. However, in this case, due to the high correlation across co-located sites (**Figure S5, Figure S6**), a LOBD CV is likely to produce more robust results. Models were generated for all combinations of training and test data.

Note that for simple linear regressions, overfitting is not an issue and no CV is required.

# S3: Supplementary Tables

***Table S1****: Site location of each Love My Air sensor, as well as summary statistics of minute-level measurements from the co-located sensors included in the analysis*

| | | | | | $PM_{2.5}$ (μg/m³) | | | Temperature (⁰C) | RH (%) | Dewpoint (⁰C) |
|---|---|---|---|---|---|---|---|---|---|---|
| **Sensor ID** | **Co-location Information** | **Latitude** | **Longitude** | **Minutes operational** | **Mean** | **Median** | **Min-Max** | **Mean** | **Mean** | **Mean** |
| **CS2** | Co-located at I25 Globeville | 39.786 | -104.989 | 211,770 | 15 | 11 | 0 - 207 | 24.2 | 60.1 | 14.2 |
| **CS5** | Co-located at La Casa | 39.779 | -105.005 | 190,531 | 14 | 10 | 0 - 209 | 21.7 | 66.5 | 13.1 |
| **CS13** | Co-located at CAMP | 39.751 | -104.988 | 206,969 | 14 | 10 | 0 - 177 | 25.7 | 52.2 | 13.1 |
| **CS16** | Co-located at I25 Denver | 39.732 | -105.015 | 206,338 | 14 | 11 | 0 - 303 | 25.6 | 30.8 | 3.5 |

***Table S2****: Performance of the calibration models using corrections C3 and C4 as captured using root mean square error (RMSE), and Pearson correlation (R) over the weeks of co-location alone. LOSO CV was used to prevent overfitting in the machine learning models*

| **ID** | **Name** | **Model** | **C3** *Correction developed using measurements made in the first two weeks of January* **(1318 measurements)** | | **C4** *Correction developed using measurements from the first two weeks of January and the first two weeks in May* **(2973 measurements)** | |
|---|---|---|---|---|---|---|
| | | | **R** | **RMSE** (μg/m³) | **R** | **RMSE** (μg/m³) |
| | **Raw Love My Air measurements** | | | | | |
| 0 | Raw | | 0.907 | 5.008 | 0.898 | 3.983 |
| | **Multivariate Regression (LOSO CV)** | | | | | |
| 1 | Linear | $PM_{2.5,\ corrected} = PM_{2.5} \times s1 + b$ | 0.907 | 3.244 | 0.898 | 2.591 |
| 2 | +RH | $PM_{2.5,\ corrected} = PM_{2.5} \times s_1 + RH \times s_2 + b$ | 0.915 | 3.110 | 0.909 | 2.453 |
| 3 | +T | $PM_{2.5,\ corrected} = PM_{2.5} \times s_1 + T \times s_2 + b$ | 0.909 | 3.206 | 0.900 | 2.567 |
| 4 | +D | $PM_{2.5,\ corrected} = PM_{2.5} \times s_1 + D \times s_2 + b$ | 0.910 | 3.199 | 0.899 | 2.568 |
| 5 | +RH x T | $PM_{2.5,\ corrected} = PM_{2.5} \times s_1 + RH \times s_2 + T \times s_3 + RH \times T \times s_4 + b$ | 0.915 | 3.103 | 0.911 | 2.424 |
| 6 | +RH x D | $PM_{2.5,\ corrected} = PM_{2.5} \times s_1 + RH \times s_2 + D \times s_3 + RH \times D \times s_4 + b$ | 0.916 | 3.087 | 0.909 | 2.451 |

| | | | | | | |
|---|---|---|---|---|---|---|
| 7 | +D x T | $PM_{2.5, corrected} = PM_{2.5} \times s_1 + D \times s_2 + T \times s_3 + D \times T \times s_4 + b$ | 0.914 | 3.118 | 0.908 | 2.457 |
| 8 | +RH x T x D | $PM_{2.5, corrected} = PM_{2.5} \times s_1 + RH \times s_2 + T \times s_3 + D \times s_4 + RH \times T \times s_5 + RH \times D \times s_6 + T \times D \times s_7 + RH \times T \times D \times s_8 + b$ | 0.918 | 3.051 | 0.914 | 2.385 |
| 9 | PM x RH | $PM_{2.5, corrected} = PM_{2.5} \times s_1 + RH \times s_2 + RH \times PM_{2.5} \times s_3 + b$ | 0.918 | 3.051 | 0.913 | 2.402 |
| 10 | PM x D | $PM_{2.5, corrected} = PM_{2.5} \times s_1 + D \times s_2 + D \times PM_{2.5} \times s_3 + b$ | 0.911 | 3.179 | 0.901 | 2.555 |
| 11 | PM x T | $PM_{2.5, corrected} = PM_{2.5} \times s_1 + T \times s_2 + T \times PM_{2.5} \times s_3 + b$ | 0.911 | 3.169 | 0.900 | 2.567 |
| 12 | PM x nonlinear RH | $PM_{2.5, corrected} = PM_{2.5} \times s_1 + \frac{RH^2}{(1-RH)} \times s_2 + \frac{RH^2}{(1-RH)} \times PM_{2.5} \times s_3 + b$ | 0.926 | 2.898 | 0.920 | 2.299 |
| 13 | PM x RH x T | $PM_{2.5, corrected} = PM_{2.5} \times s_1 + RH \times s_2 + T \times s_3 + PM_{2.5} \times RH \times s_4 + PM_{2.5} \times T \times s_5 + RH \times T \times s_6 + PM_{2.5} \times RH \times T \times s_7 + b$ | 0.919 | 3.041 | 0.914 | 2.383 |
| 14 | PM x RH x D | $PM_{2.5, corrected} = PM_{2.5} \times s_1 + RH \times s_2 + D \times s_3 + PM_{2.5} \times RH \times s_4 + PM_{2.5} \times D \times s_5 + RH \times D \times s_6 + PM_{2.5} \times RH \times D \times s_7 + b$ | 0.920 | 3.013 | 0.914 | 2.388 |
| 15 | PM x T x D | $PM_{2.5, corrected} = PM_{2.5} \times s_1 + T \times s_2 + D \times s_3 + PM_{2.5} \times T \times s_4 + PM_{2.5} \times D \times s_5 + T \times D \times s_6 + PM_{2.5} \times T \times D \times s_7 + b$ | 0.919 | 3.035 | 0.913 | 2.403 |
| 16 | PM x RH x T x D | $PM_{2.5, corrected} = PM_{2.5} \times s_1 + RH \times s_2 + T \times s_3 + D \times s_4 + PM_{2.5} \times RH \times s_5 + PM_{2.5} \times T \times s_6 + T \times RH \times s_7 + PM_{2.5} \times D \times s_8 + D \times RH \times s_9 + D \times T \times s_{10} + PM_{2.5} \times RH \times T \times s_{11} + PM_{2.5} \times RH \times D \times s_{12} + PM_{2.5} \times D \times T \times s_{13} + D \times RH \times T \times s_{14} + PM_{2.5} \times RH \times T \times D \times s_{15} + b$ | 0.931 | 2.813 | 0.921 | 2.295 |
| | **Machine Learning (LOSO CV)** | | | | | |
| 17 | Random Forest | $PM_{2.5, corrected} = f(PM_{2.5}, T, RH)$ | 0.982 | 1.506 | 0.978 | 1.234 |
| 18 | Neural Network (One hidden layer) | $PM_{2.5, corrected} = f(PM_{2.5}, T, RH)$ | 0.918 | 3.049 | | |

| | | | | | | |
|---|---|---|---|---|---|---|
| 19 | Gradient Boosting | $PM_{2.5, corrected} = f(PM_{2.5}, T, RH)$ | 0.938 | 2.683 | 0.926 | 2.225 |
| 20 | SuperLearner | $PM_{2.5, corrected} = f(PM_{2.5}, T, RH)$ | 0.954 | 2.309 | 0.925 | 2.238 |
| 21 | Random Forest | $PM_{2.5, corrected} = f(PM_{2.5}, T, RH, D, cos\_time)$ | 0.983 | 1.548 | 0.962 | 1.607 |

***Table S3**: Performance of the calibration models as captured using root mean square error (RMSE), normalized RMSE, and Pearson correlation (R) for true $PM_{2.5}$ > 30 μg/m$^3$ and $PM_{2.5}$ ≤ 30 μg/m$^3$. LOSO CV was used to prevent overfitting in the machine learning models*

| | | | **$PM_{2.5}$ > 30 μg/m$^3$ (n = 1038 measurements)** | | | | | | | | **$PM_{2.5}$ ≤ 30 μg/m$^3$ (n=26300 measurements)** | | | | | | | |
|---|---|---|---|---|---|---|---|---|---|---|---|---|---|---|---|---|---|---|
| **ID** | **Name** | **Model** | **C1** *Correction developed on data during the entire period of network operation* | | **C2** *On-the-fly correction developed using data for the same week of measurement* | | **C3** *Correction developed using measurements made in the first two weeks of January* | | **C4** *Correction developed using measurements from the first two weeks of January and the first two weeks in May* | | **C1** *Correction developed on data during the entire period of network operation* | | **C2** *On-the-fly correction developed using data for the same week of measurement* | | **C3** *Correction developed using measurements made in the first two weeks of January* | | **C4** *Correction developed using measurements from the first two weeks of January and the first two weeks in May* | |
| | | | **R** | **RMSE (nRMSE)** | **R** | **RMSE (nRMSE)** | **R** | **RMSE (nRMSE)** | **R** | **RMSE (nRMSE)** | **R** | **RMSE (nRMSE)** | **R** | **RMSE (nRMSE)** | **R** | **RMSE (nRMSE)** | **R** | **RMSE (nRMSE)** |
| | **Raw Love My Air measurements** | | | | | | | | | | | | | | | | | |
| 0 | Raw | | 0.797 | 14.928 (0.350) | - | - | - | - | - | - | 0.915 | 5.891 (0.646) | - | - | - | - | - | - |
| | **Multivariate Regression (LOSO CV)** | | | | | | | | | | | | | | | | | |
| 1 | Linear | $PM_{2.5, corrected} = PM_{2.5} \times s1 + b$ | 0.797 | 11.263 (0.264) | 0.834 | 9.522 (0.223) | 0.797 | 10.556 (0.248) | 0.797 | 11.105 (0.260) | 0.915 | 2.676 (0.294) | 0.921 | 2.414 (0.265) | 0.915 | 2.869 (0.315) | 0.915 | 2.705 (0.297) |
| 2 | +RH | $PM_{2.5, corrected} = PM_{2.5} \times s_1 + RH \times s_2 + b$ | 0.802 | 11.083 (0.260) | 0.838 | 9.316 (0.218) | 0.806 | 9.379 (0.220) | 0.804 | 9.979 (0.234) | 0.917 | 2.650 (0.291) | 0.927 | 2.311 (0.254) | 0.913 | 3.184 (0.349) | 0.915 | 2.921 (0.320) |
| 3 | +T | $PM_{2.5, corrected} = PM_{2.5} \times s_1 + T \times s_2 + b$ | 0.799 | 11.219 (0.263) | 0.839 | 9.246 (0.217) | 0.803 | 9.395 (0.220) | 0.801 | 10.418 (0.244) | 0.916 | 2.667 (0.293) | 0.928 | 2.311 (0.254) | 0.911 | 3.567 (0.391) | 0.915 | 2.856 (0.313) |
| 4 | +D | $PM_{2.5, corrected} = PM_{2.5} \times s_1 + D \times s_2 + b$ | 0.797 | 11.267 (0.264) | 0.841 | 9.285 (0.218) | 0.791 | 11.339 (0.266) | 0.795 | 11.361 (0.266) | 0.916 | 2.670 (0.293) | 0.925 | 2.354 (0.258) | 0.895 | 3.043 (0.334) | 0.910 | 2.724 (0.299) |
| 5 | +RH x T | $PM_{2.5, corrected} = PM_{2.5} \times s_1 + RH \times s_2 + T \times s_3 + RH \times T \times$ | 0.806 | 10.772 (0.253) | 0.852 | 8.866 (0.208) | 0.804 | 9.636 (0.226) | 0.806 | 9.868 (0.231) | 0.923 | 2.543 (0.279) | 0.933 | 2.224 (0.244) | 0.917 | 2.954 (0.324) | 0.922 | 2.790 (0.306) |

| | | | | | | | | | | | | | | | | | | |
|---|---|---|---|---|---|---|---|---|---|---|---|---|---|---|---|---|---|---|
| | | $s_4 + b$ | | | | | | | | | | | | | | | | |
| 6 | +RH x D | $PM_{2.5,\ corrected} = PM_{2.5} \times s_1 + RH \times s_2 + D \times s_3 + RH \times D \times s_4 + b$ | 0.803 | 11.031<br>(0.259) | 0.848 | 8.896<br>(0.209) | 0.803 | 9.598<br>(0.225) | 0.804 | 9.883<br>(0.232) | 0.918 | 2.635<br>(0.289) | 0.933 | 2.222<br>(0.244) | 0.886 | 3.573<br>(0.392) | 0.916 | 2.932<br>(0.322) |
| 7 | +D x T | $PM_{2.5,\ corrected} = PM_{2.5} \times s_1 + D \times s_2 + T \times s_3 + D \times T \times s_4 + b$ | 0.799 | 11.211<br>(0.263) | 0.847 | 8.946<br>(0.210) | 0.789 | 8.981<br>(0.211) | 0.798 | 10.033<br>(0.235) | 0.916 | 2.668<br>(0.293) | 0.933 | 2.231<br>(0.245) | 0.863 | 5.529<br>(0.607) | 0.908 | 3.226<br>(0.354) |
| 8 | +RH x T x D | $PM_{2.5,\ corrected} = PM_{2.5} \times s_1 + RH \times s_2 + T \times s_3 + D \times s_4 + RH \times T \times s_5 + RH \times D \text{ x } s_6 + T \times D \times s_7 + RH \times T \times D \times s_8 + b$ | 0.809 | 10.723<br>(0.251) | 0.853 | 8.713<br>(0.204) | 0.746 | 10.822<br>(0.254) | 0.795 | 9.981<br>(0.234) | 0.924 | 2.532<br>(0.278) | 0.936 | 2.172<br>(0.238) | 0.700 | 6.887<br>(0.756) | 0.915 | 3.119<br>(0.342) |
| 9 | PM x RH | $PM_{2.5,\ corrected} = PM_{2.5} \times s_1 + RH \times s_2 + RH \times PM_{2.5} \times s_3 + b$ | 0.811 | 10.943<br>(0.257) | 0.839 | 9.224<br>(0.216) | 0.807 | 8.896<br>(0.209) | 0.806 | 9.148<br>(0.214) | 0.917 | 2.651<br>(0.291) | 0.931 | 2.260<br>(0.248) | 0.908 | 3.617<br>(0.397) | 0.909 | 3.383<br>(0.371) |
| 10 | PM x D | $PM_{2.5,\ corrected} = PM_{2.5} \times s_1 + D \times s_2 + D \times PM_{2.5} \times s_3 + b$ | 0.810 | 10.640<br>(0.249) | 0.852 | 9.027<br>(0.212) | 0.710 | 15.827<br>(0.371) | 0.760 | 13.433<br>(0.315) | 0.915 | 2.649<br>(0.291) | 0.927 | 2.314<br>(0.254) | 0.860 | 3.285<br>(0.360) | 0.899 | 2.776<br>(0.305) |
| 11 | PM x T | $PM_{2.5,\ corrected} = PM_{2.5} \times s_1 + T \times s_2 + T \times PM_{2.5} \times s_3 + b$ | 0.815 | 10.813<br>(0.254) | 0.848 | 8.960<br>(0.210) | 0.771 | 12.444<br>(0.292) | 0.803 | 10.219<br>(0.240) | 0.915 | 2.675<br>(0.293) | 0.932 | 2.243<br>(0.246) | 0.879 | 6.159<br>(0.676) | 0.915 | 2.892<br>(0.317) |
| 12 | PM x nonlinear RH | $PM_{2.5,\ corrected} = PM_{2.5} \times s_1 + \frac{RH^2}{(1-RH)} \times s_2 + \frac{RH^2}{(1-RH)} \times PM_{2.5} \times s_3 + b$ | 0.821 | 10.695<br>(0.251) | 0.844 | 9.157<br>(0.215) | 0.815 | 9.322<br>(0.219) | 0.814 | 9.712<br>(0.228) | 0.923 | 2.579<br>(0.283) | 0.927 | 2.331<br>(0.256) | 0.920 | 3.063<br>(0.336) | 0.920 | 2.884<br>(0.316) |
| 13 | PM x RH x T | $PM_{2.5,\ corrected} = PM_{2.5} \times s_1 + RH \times s_2 + T \times s_3 + PM_{2.5} \times RH \times s_4 + PM_{2.5} \times T \times s_5 + RH \times T \times s_6 + PM_{2.5} \times RH \times T \times s_7 + b$ | 0.816 | 10.337<br>(0.242) | 0.860 | 8.584<br>(0.201) | 0.736 | 12.672<br>(0.297) | 0.799 | 10.155<br>(0.238) | 0.926 | 2.489<br>(0.273) | 0.939 | 2.124<br>(0.233) | 0.860 | 5.820<br>(0.639) | 0.916 | 2.940<br>(0.323) |
| 14 | PM x RH x D | $PM_{2.5,\ corrected} = PM_{2.5} \times s_1 + RH \times s_2 + D \times s_3 + PM_{2.5} \times RH \times s_4 + PM_{2.5} \times D \times s_5 + RH \times D \times s_6 + PM_{2.5} \times RH \times D \times s_7 + b$ | 0.817 | 10.496<br>(0.246) | 0.860 | 8.528<br>(0.200) | 0.677 | 16.862<br>(0.395) | 0.775 | 9.830<br>(0.230) | 0.917 | 2.624<br>(0.288) | 0.939 | 2.121<br>(0.233) | 0.850 | 6.634<br>(0.728) | 0.901 | 3.618<br>(0.397) |
| 15 | PM x T x D | $PM_{2.5,\ corrected} = PM_{2.5} \times s_1 + T \times s_2 + D \times s_3 + PM_{2.5} \times T \times s_4 + PM_{2.5} \times D \times s_5 + T \times D \times s_6 + PM_{2.5} \times T \times D \times s_7 + b$ | 0.813 | 10.575<br>(0.248) | 0.860 | 8.543<br>(0.200) | 0.529 | 21.253<br>(0.498) | 0.760 | 9.819<br>(0.230) | 0.915 | 2.648<br>(0.291) | 0.939 | 2.122<br>(0.233) | 0.700 | 4.843<br>(0.531) | 0.889 | 4.236<br>(0.465) |
| 16 | PM x RH x T x D | $PM_{2.5,\ corrected} = PM_{2.5} \times s_1 + RH \times s_2 + T \times s_3 + D \times s_4 + PM_{2.5} \times RH \times s_5 + PM_{2.5} \times T \text{ x } s_6 + T \times RH \times s_7 + PM_{2.5} \times D \times s_8 + D \times RH \times s_9 + D \times T \times s_{10} + PM_{2.5} \times RH \times T \times s_{11} + PM_{2.5} \times RH \times D \times s_{12} + PM_{2.5} \times D \times T \times s_{13} + D \times RH \times T \times s_{14} + PM_{2.5} \times RH \times$ | 0.829 | 10.017<br>(0.235) | 0.872 | 8.103<br>(0.190) | 0.204 | 81.527<br>(1.911) | 0.723 | 12.778<br>(0.300) | 0.926 | 2.475<br>(0.272) | 0.943 | 2.050<br>(0.225) | 0.317 | 29.433<br>(3.229) | 0.702 | 6.392<br>(0.701) |

| | | | | | | | | | | | | | | | | | | |
|---|---|---|---|---|---|---|---|---|---|---|---|---|---|---|---|---|---|---|
| | | $T \times D \times s_{15} + b$ | | | | | | | | | | | | | | | | |
| | **Machine Learning (LOSO CV)** | | | | | | | | | | | | | | | | | |
| 17 | Random Forest | $PM_{2.5,\ corrected}$ = f($PM_{2.5}$, T, RH) | 0.940 | 5.380 (0.126) | 0.953 | 4.670 (0.109) | 0.651 | 13.773 (0.323) | 0.610 | 15.006 (0.352) | 0.973 | 1.382 (0.152) | 0.982 | 1.151 (0.126) | 0.903 | 2.922 (0.321) | 0.917 | 2.513 (0.276) |
| 18 | Neural Network (One hidden layer) | $PM_{2.5,\ corrected}$ = f($PM_{2.5}$, T, RH) | 0.808 | 10.246 (0.240) | 0.855 | 8.914 (0.209) | 0.815 | 9.994 (0.234) | 0.678 | 12.079 (0.283) | 0.902 | 2.661 (0.292) | 0.920 | 2.388 (0.262) | 0.905 | 3.026 (0.332) | 0.878 | 4.177 (0.458) |
| 19 | Gradient Boosting | $PM_{2.5,\ corrected}$ = f($PM_{2.5}$, T, RH) | 0.849 | 9.122 (0.214) | 0.888 | 7.583 (0.178) | 0.546 | 13.086 (0.307) | 0.521 | 13.195 (0.309) | 0.926 | 2.298 (0.252) | 0.944 | 1.995 (0.219) | 0.899 | 2.946 (0.323) | 0.897 | 2.899 (0.318) |
| 20 | SuperLearner | $PM_{2.5,\ corrected}$ = f($PM_{2.5}$, T, RH) | 0.854 | 8.912 (0.209) | 0.923 | 6.359 (0.149) | 0.636 | 12.740 (0.299) | 0.676 | 12.139 (0.285) | 0.926 | 2.311 | 0.950 | 1.898 (0.208) | 0.898 | 3.089 (0.339) | 0.910 | 2.743 (0.301) |
| 21 | Random Forest | For corrections C1 $PM_{2.5,\ corrected}$ = f($PM_{2.5}$, T, RH, D, cos_time, cos_month, sin_month)<br><br>For corrections C2, C3, C4 $PM_{2.5,\ corrected}$ = f($PM_{2.5}$, T, RH, D, cos_time) | 0.951 | 4.819 (0.113) | 0.962 | 4.180 (0.098) | 0.512 | 20.913 (0.490) | 0.536 | 19.551 (0.458) | 0.926 | 2.311 (0.254) | 0.986 | 1.018 (0.112) | 0.882 | 3.011 (0.330) | 0.897 | 2.659 (0.292) |

***Table S4**: Performance of the calibration models using the C1 correction as captured using root mean square error (RMSE), normalized RMSE, and Pearson correlation (R) for true $PM_{2.5}$ > 30 μg/m$^3$ and $PM_{2.5}$ ≤ 30 μg/m$^3$. LOBD CV was used to prevent overfitting in the machine learning models*

| | | | **$PM_{2.5}$ > 30 μg/m$^3$ (n = 1038 measurements)** | | **$PM_{2.5}$ ≤ 30 μg/m$^3$ (n=27338 measurements)** | |
|---|---|---|---|---|---|---|
| **ID** | **Machine Learning (LOBD CV)** | | **R** | **RMSE (μg/m$^3$)** | **R** | **RMSE (μg/m$^3$)** |
| 17 | Random Forest | $PM_{2.5,\ corrected}$ = f($PM_{2.5}$, T, RH) | 0.939 | 5.415 (0.127) | 0.974 | 1.372 (0.151) |
| 18 | Neural Network (One hidden layer) | $PM_{2.5,\ corrected}$ = f($PM_{2.5}$, T, RH) | 0.808 | 10.200 (0.239) | 0.902 | 2.666 (0.293) |
| 19 | Gradient Boosting | $PM_{2.5,\ corrected}$ = f($PM_{2.5}$, T, RH) | 0.863 | 8.536 (0.200) | 0.930 | 2.245 (0.246) |
| 20 | SuperLearner | $PM_{2.5,\ corrected}$ = f($PM_{2.5}$, T, RH) | 0.885 | 7.988 (0.187) | 0.930 | 2.240 (0.246) |
| 21 | Random Forest | $PM_{2.5,\ corrected}$ = f($PM_{2.5}$, T, RH, D, cos_time, cos_month, sin_month) | 0.952 | 4.724 (0.111) | 0.981 | 1.181 (0.130) |

***Table S5**: Performance of the calibration models developed using the co-located hourly measurements to the minute-level data as captured using root mean square error (RMSE), and Pearson correlation (R). LOSO CV was used to prevent overfitting in the machine learning models. All corrected values were evaluated over the entire time period (April 23 - September 30, 2021).*

| ID | Name | Model | **C1** *Correction developed on data during the entire period of network operation* | | **C2** *On-the-fly correction developed using data for the same week of measurement* | | **C3** *Correction developed using measurements made in the first two weeks of January* | | **C4** *Correction developed using measurements from the first two weeks of January and the first two weeks in May* | |
|---|---|---|---|---|---|---|---|---|---|---|
| | | | **R** | **RMSE ($\mu g/m^3$)** | **R** | **RMSE ($\mu g/m^3$)** | **R** | **RMSE ($\mu g/m^3$)** | **R** | **RMSE ($\mu g/m^3$)** |
| | **Raw Love My Air measurements** | | | | | | | | | |
| 0 | Raw | | 0.497 | 16.409 | - | - | - | - | - | - |
| | **Multivariate Regression (LOSO CV)** | | | | | | | | | |
| 1 | Linear | $PM_{2.5, corrected} = PM_{2.5} \times s1 + b$ | 0.497 | 15.667 | 0.498 | 15.646 | 0.497 | 15.657 | 0.497 | 15.663 |
| 2 | +RH | $PM_{2.5, corrected} = PM_{2.5} \times s_1 + RH \times s_2 + b$ | 0.495 | 15.678 | 0.500 | 15.618 | 0.492 | 15.721 | 0.494 | 15.686 |
| 3 | +T | $PM_{2.5, corrected} = PM_{2.5} \times s_1 + T \times s_2 + b$ | 0.496 | 15.670 | 0.500 | 15.621 | 0.493 | 15.822 | 0.495 | 15.671 |
| 4 | +D | $PM_{2.5, corrected} = PM_{2.5} \times s_1 + D \times s_2 + b$ | 0.497 | 15.663 | 0.498 | 15.640 | 0.491 | 15.805 | 0.495 | 15.693 |
| 5 | +RH x T | $PM_{2.5, corrected} = PM_{2.5} \times s_1 + RH \times s_2 + T \times s_3 + RH \times T \times s_4 + b$ | 0.499 | 15.634 | 0.500 | 15.621 | 0.495 | 15.669 | 0.498 | 15.640 |
| 6 | +RH x D | $PM_{2.5, corrected} = PM_{2.5} \times s_1 + RH \times s_2 + D \times s_3 + RH \times D \times s_4 + b$ | 0.496 | 15.671 | 0.500 | 15.622 | 0.477 | 15.892 | 0.494 | 15.684 |
| 7 | +D x T | $PM_{2.5, corrected} = PM_{2.5} \times s_1 + D \times s_2 + T \times s_3 + D \times T \times s_4 + b$ | 0.470 | 15.928 | 0.014 | 323.684 | 0.018 | 257.153 | 0.032 | 135.647 |
| 8 | +RH x T x D | $PM_{2.5, corrected} = PM_{2.5} \times s_1 + RH \times s_2 + T \times s_3 + D \times s_4 + RH \times T \times s_5$ | 0.138 | 33.817 | 0.041 | 111.569 | 0.029 | 160.447 | 0.027 | 160.963 |

| | | | | | | | | | | |
|---|---|---|---|---|---|---|---|---|---|---|
| | | $+ RH \times D \times s_6 + T \times D \times s_7 + RH \times T \times D \times s_8 + b$ | | | | | | | | |
| 9 | PM x RH | $PM_{2.5, corrected} = PM_{2.5} \times s_1 + RH \times s_2 + RH \times PM_{2.5} \times s_3 + b$ | 0.494 | 15.688 | 0.501 | 15.615 | 0.485 | 15.896 | 0.486 | 15.844 |
| 10 | PM x D | $PM_{2.5, corrected} = PM_{2.5} \times s_1 + D \times s_2 + D \times PM_{2.5} \times s_3 + b$ | 0.498 | 15.644 | 0.499 | 15.630 | 0.477 | 16.145 | 0.491 | 15.820 |
| 11 | PM x T | $PM_{2.5, corrected} = PM_{2.5} \times s_1 + T \times s_2 + T \times PM_{2.5} \times s_3 + b$ | 0.495 | 15.675 | 0.501 | 15.610 | 0.483 | 17.172 | 0.495 | 15.675 |
| 12 | PM x nonlinear RH | $PM_{2.5, corrected} = PM_{2.5} \times s_1 + \frac{RH^2}{(1-RH)} \times s_2 + \frac{RH^2}{(1-RH)} \times PM_{2.5} \times s_3 + b$ | 0.496 | 15.659 | 0.497 | 15.650 | 0.494 | 15.705 | 0.495 | 15.681 |
| 13 | PM x RH x T | $PM_{2.5, corrected} = PM_{2.5} \times s_1 + RH \times s_2 + T \times s_3 + PM_{2.5} \times RH \times s_4 + PM_{2.5} \times T \times s_5 + RH \times T \times s_6 + PM_{2.5} \times RH \times T \times s_7 + b$ | 0.501 | 15.611 | 0.502 | 15.601 | 0.462 | 17.111 | 0.489 | 15.732 |
| 14 | PM x RH x D | $PM_{2.5, corrected} = PM_{2.5} \times s_1 + RH \times s_2 + D \times s_3 + PM_{2.5} \times RH \times s_4 + PM_{2.5} \times D \times s_5 + RH \times D \times s_6 + PM_{2.5} \times RH \times D \times s_7 + b$ | 0.496 | 15.657 | 0.502 | 15.602 | 0.460 | 17.710 | 0.479 | 15.948 |
| 15 | PM x T x D | $PM_{2.5, corrected} = PM_{2.5} \times s_1 + T \times s_2 + D \times s_3 + PM_{2.5} \times T \times s_4 + PM_{2.5} \times D \times s_5 + T \times D \times s_6 + PM_{2.5} \times T \times D \times s_7 + b$ | 0.134 | 35.196 | 0.020 | 217.684 | 0.012 | 178.589 | 0.044 | 114.530 |
| 16 | PM x RH x T x D | $PM_{2.5, corrected} = PM_{2.5} \times s_1 + RH \times s_2 + T \times s_3 + D \times s_4 + PM_{2.5} \times RH \times s_5 + PM_{2.5} \times T \times s_6 + T \times RH \times s_7 + PM_{2.5} \times D \times s_8 + D \times RH \times s_9 + D \times T \times s_{10} + PM_{2.5} \times RH \times T \times s_{11} + PM_{2.5} \times RH \times D \times s_{12} + PM_{2.5} \times D \times T \times s_{13} + D \times RH \times T \times s_{14} + PM_{2.5} \times RH \times T \times D \times s_{15} + b$ | 0.112 | 41.795 | 0.029 | 159.921 | 0.010 | 482.333 | 0.019 | 203.714 |
| | **Machine Learning (LOSO CV)** | | | | | | | | | |
| 17 | Random Forest | $PM_{2.5, corrected} = f(PM_{2.5}, T, RH)$ | 0.505 | 15.565 | 0.510 | 15.527 | 0.489 | 15.863 | 0.488 | 15.821 |
| 18 | Neural Network (One hidden layer) | $PM_{2.5, corrected} = f(PM_{2.5}, T, RH)$ | 0.496 | 15.669 | 0.501 | 15.611 | 0.495 | 15.699 | 0.477 | 16.202 |

| | | | | | | | | | | |
|---|---|---|---|---|---|---|---|---|---|---|
| 19 | Gradient Boosting | $PM_{2.5,\ corrected}$ = f($PM_{2.5}$, T, RH) | 0.500 | 15.625 | 0.502 | 15.604 | 0.485 | 15.779 | 0.486 | 15.765 |
| 20 | SuperLearner | $PM_{2.5,\ corrected}$ = f($PM_{2.5}$, T, RH) | 0.500 | 15.622 | 0.503 | 15.591 | 0.483 | 15.805 | 0.490 | 15.719 |
| 21 | Random Forest | For C1:<br>$PM_{2.5,\ corrected}$ = f($PM_{2.5}$, T, RH, D, cos_time, cos_month, sin_month)<br><br>For C2, C3, C4:<br>$PM_{2.5,\ corrected}$ = f($PM_{2.5}$, T, RH, D, cos_time) | 0.514 | 15.482 | 0.512 | 15.502 | 0.481 | 16.349 | 0.481 | 16.185 |

***Table S6****: Performance of the calibration models developed using the co-located hourly measurements to the minute-level data as captured using root mean square error (RMSE), and Pearson correlation (R).  LOBD CV was used to prevent overfitting in the machine learning models. All corrected values were evaluated over the entire time period (April 23 - September 30, 2021)*

| **ID** | **Machine Learning (LOBD CV)** | | **R** | **RMSE ($\mu g/m^3$)** |
|---|---|---|---|---|
| 17 | Random Forest | $PM_{2.5,\ corrected}$ = f($PM_{2.5}$, T, RH) | 0.506 | 15.561 |
| 18 | Neural Network (One hidden layer) | $PM_{2.5,\ corrected}$ = f($PM_{2.5}$, T, RH) | 0.496 | 15.666 |
| 19 | Gradient Boosting | $PM_{2.5,\ corrected}$ = f($PM_{2.5}$, T, RH) | 0.501 | 15.610 |
| 20 | SuperLearner | $PM_{2.5,\ corrected}$ = f($PM_{2.5}$, T, RH) | 0.503 | 15.594 (1.326) |
| 21 | Random Forest | $PM_{2.5,\ corrected}$ = f($PM_{2.5}$, T, RH, D, cos_time, cos_month, sin_month) | 0.510 | 15.516 |

# S4: Supplementary Figures

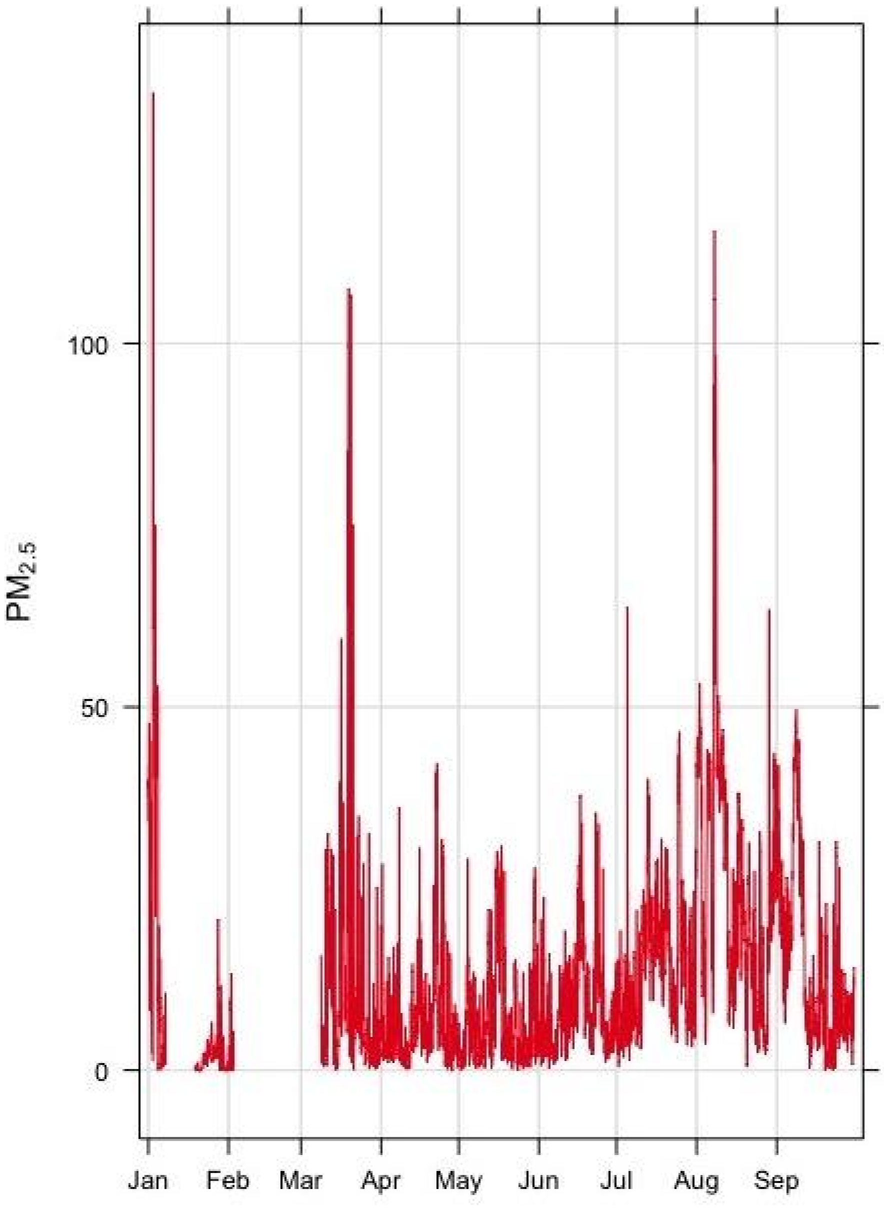


***Figure S1****: Hourly averaged $PM_{2.5}$ time-series of the Love My Air sensor CS13, co-located at the CAMP reference site*

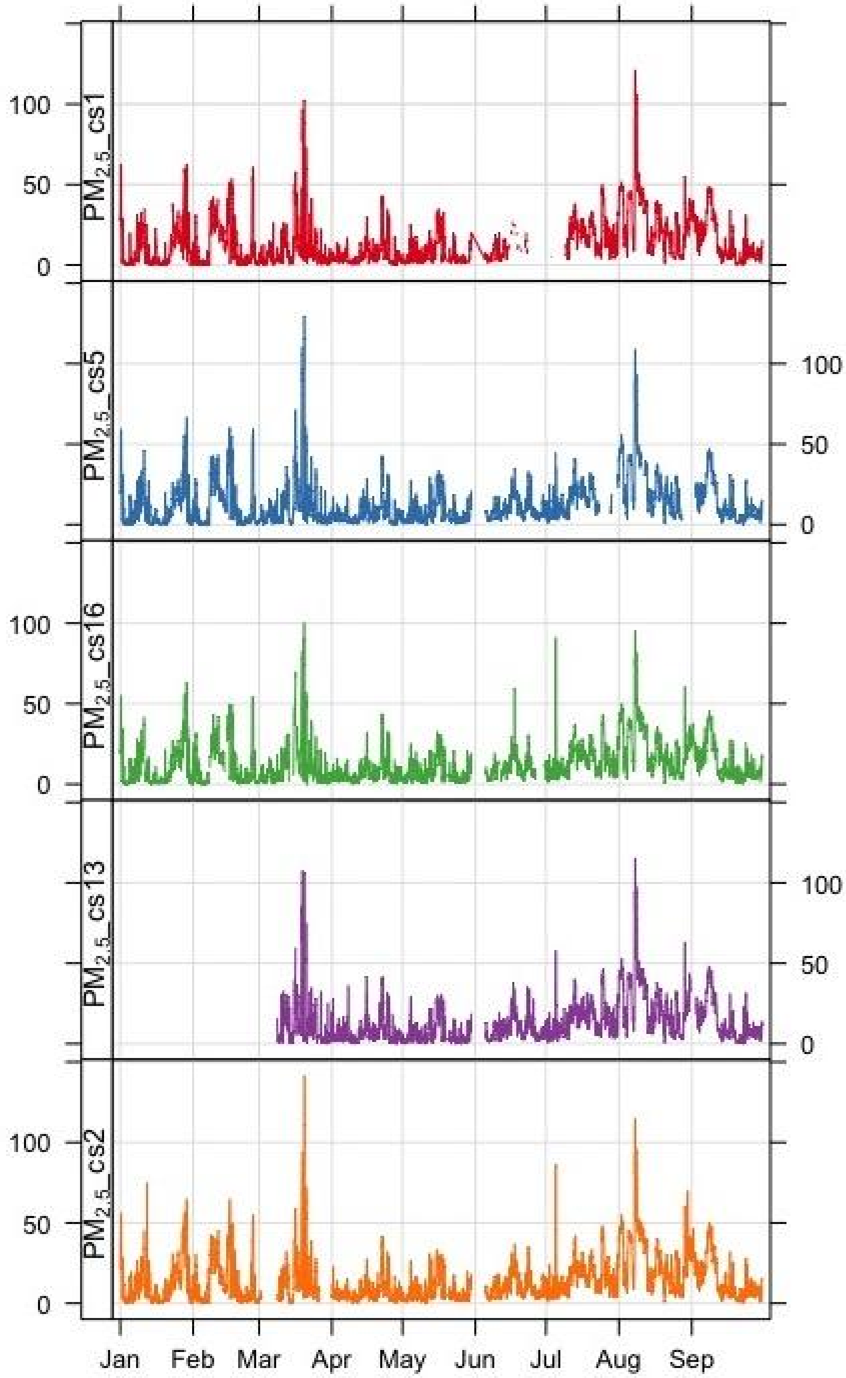


***Figure S2**: Hourly averaged $PM_{2.5}$ time-series of all Love My Air sensors co-located with reference monitors in Denver*

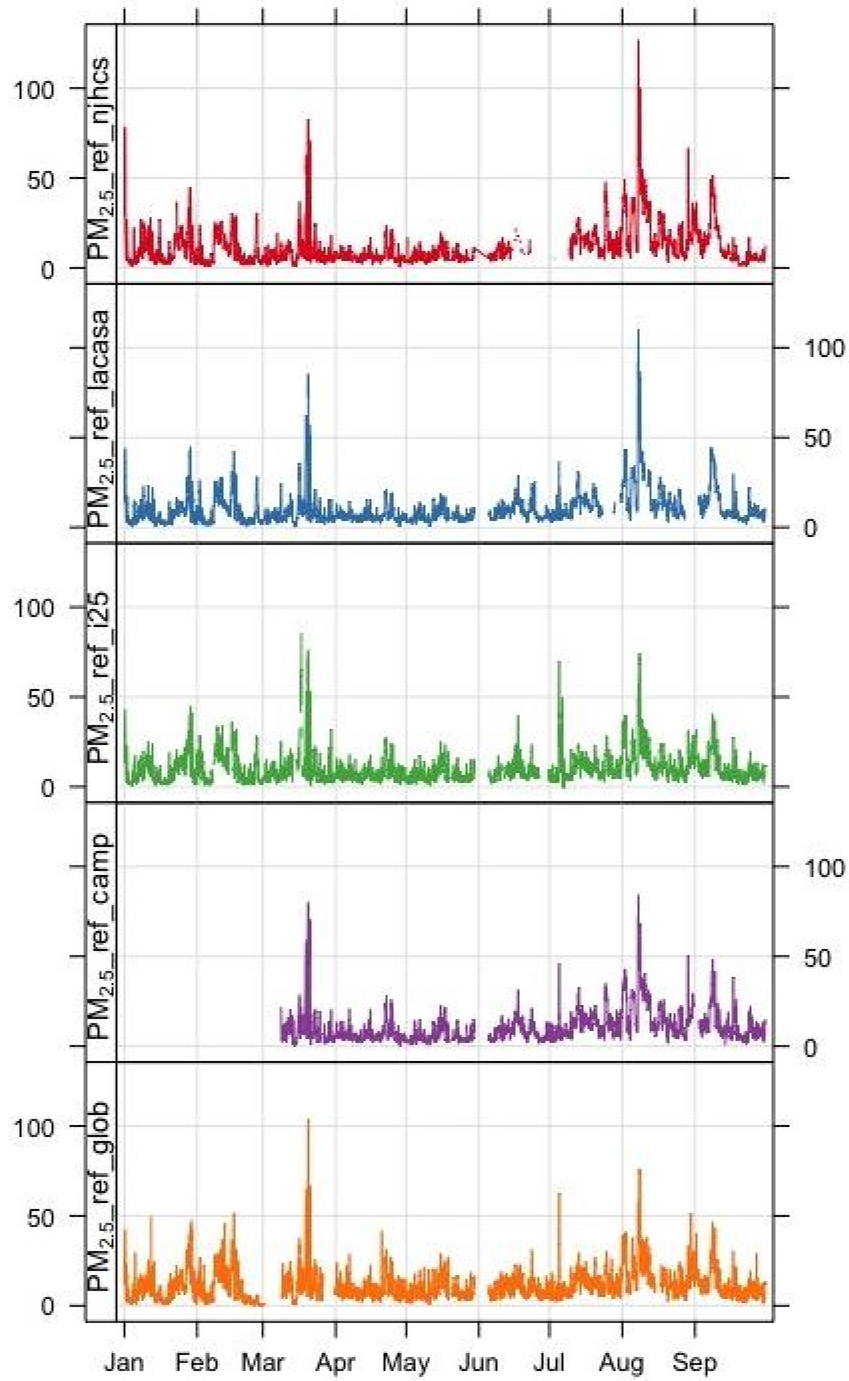


***Figure S3**: Hourly averaged $PM_{2.5}$ time-series of all reference air quality monitors in Denver*

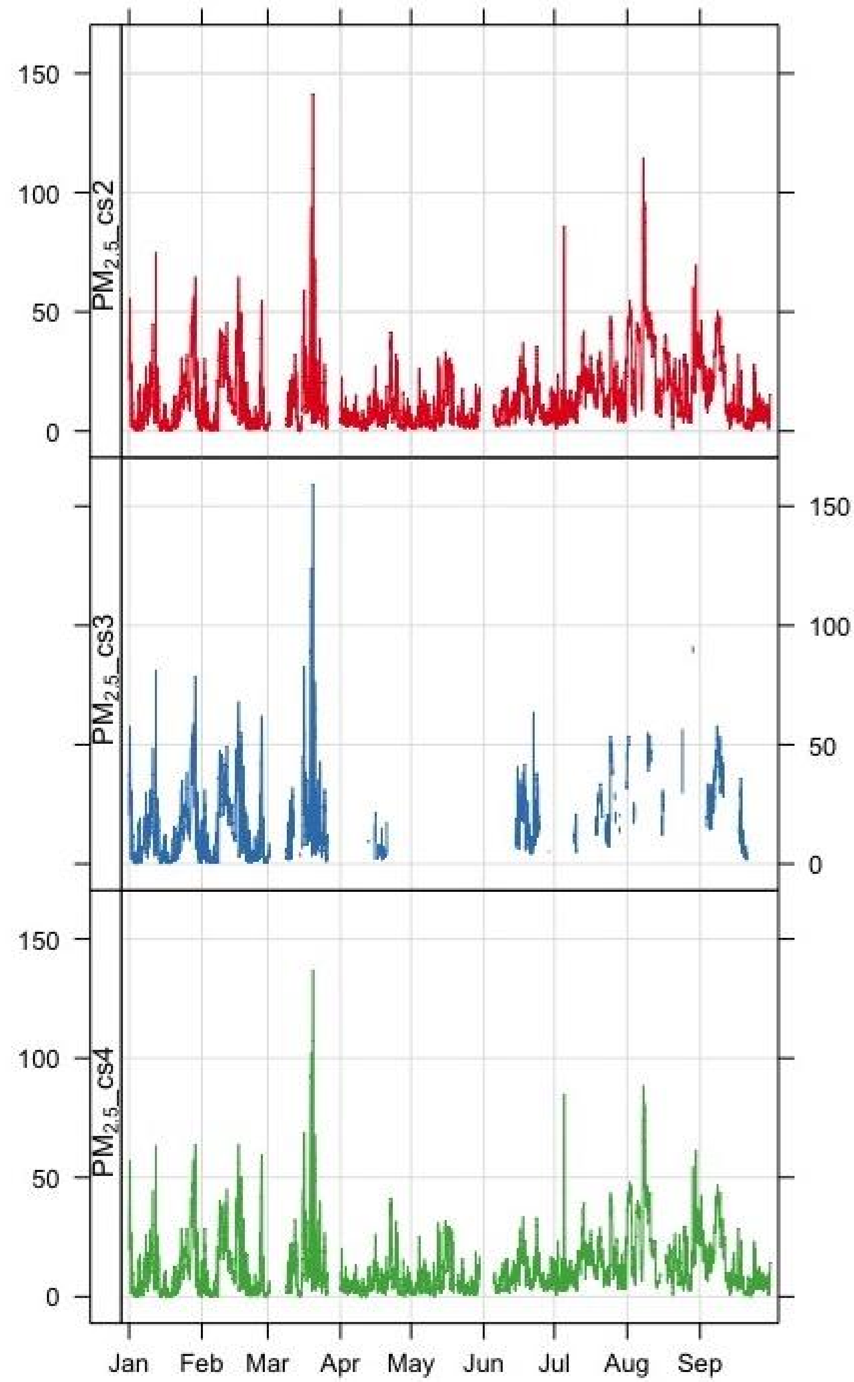


***Figure S4**: Hourly averaged $PM_{2.5}$ time-series of the Love My Air sensors CS2, CS3, and CS4, co-located at the I25 Globeville reference site*

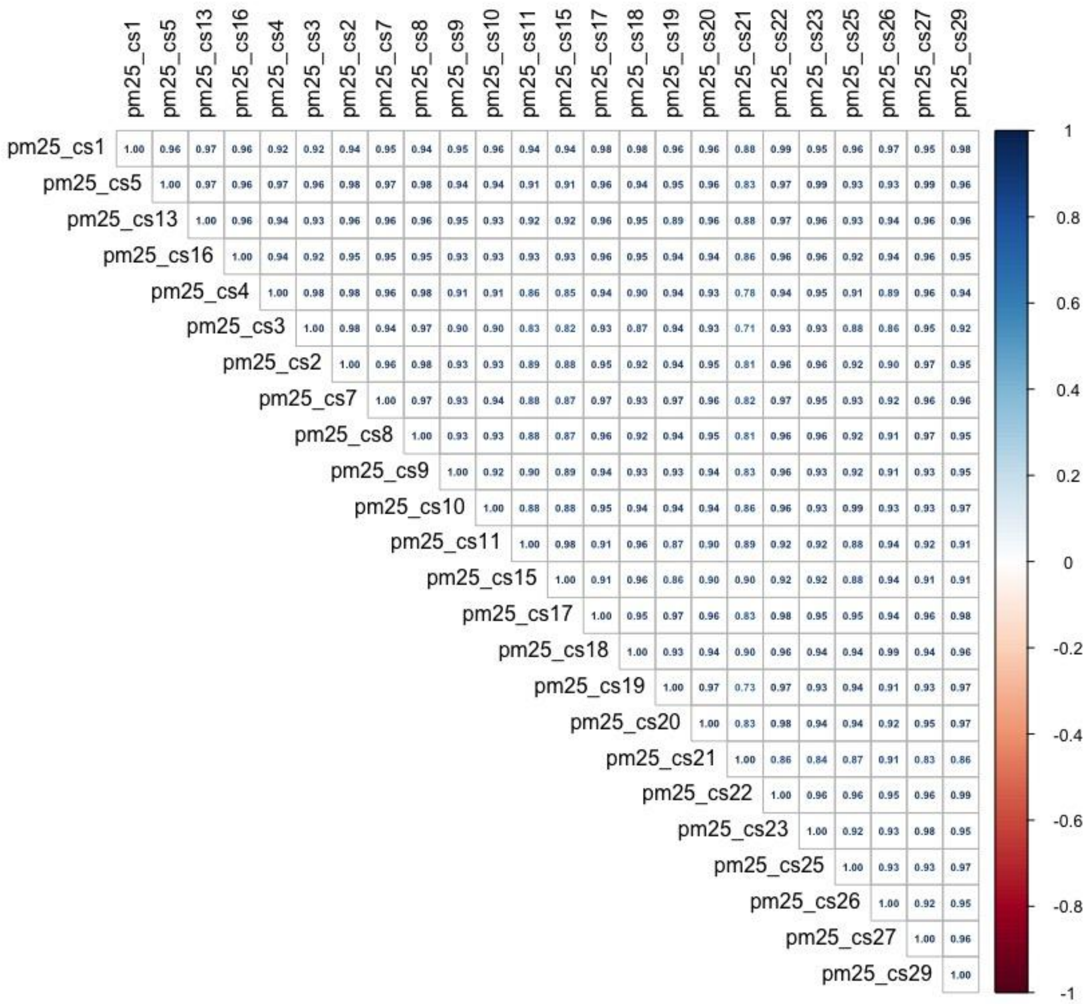


***Figure S5****: Correlations between hourly averaged $PM_{2.5}$ measurements from each Love My Air sensor in the network*

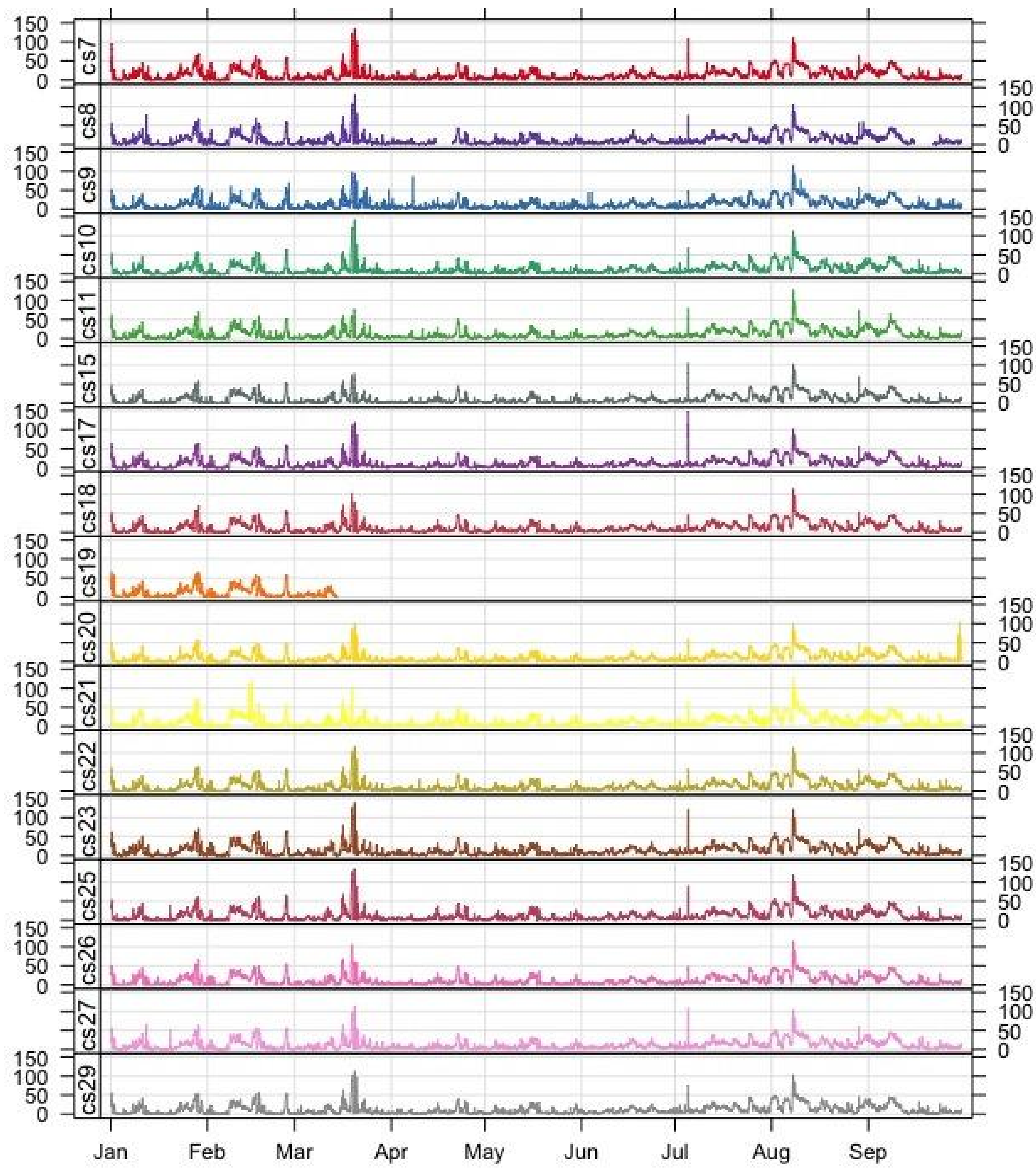


***Figure S6****: Uncorrected hourly averaged $PM_{2.5}$ time series of all Love My Air sensors not co-located with a reference monitor*

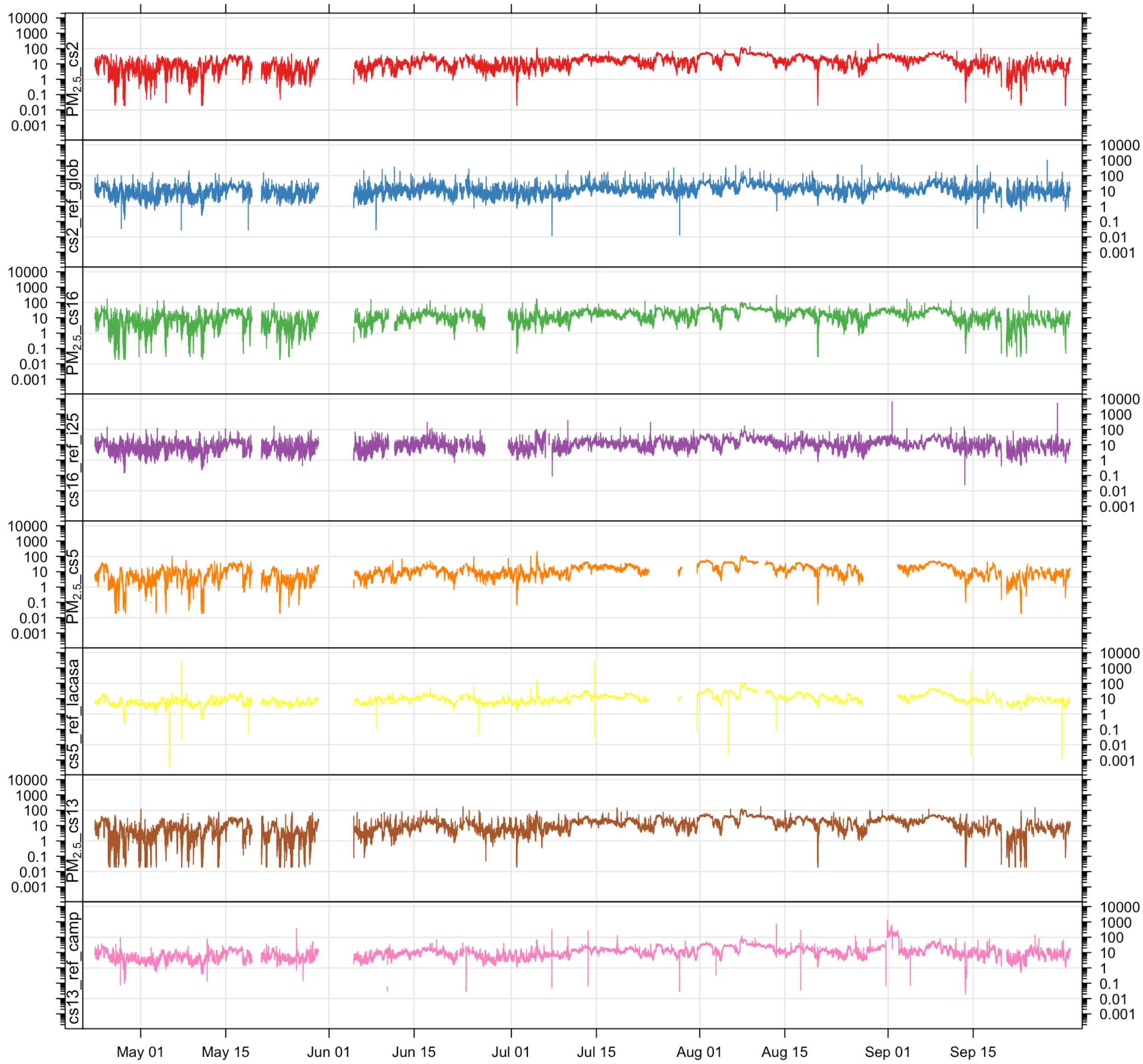


***Figure S7****: Uncorrected minute level $PM_{2.5}$ time series of Love My Air sensors co-located and minute level measurements from reference monitors at sites I25 Globeville, I25 Denver, La Casa and CAMP. The y-axis has been transformed to the log scale*

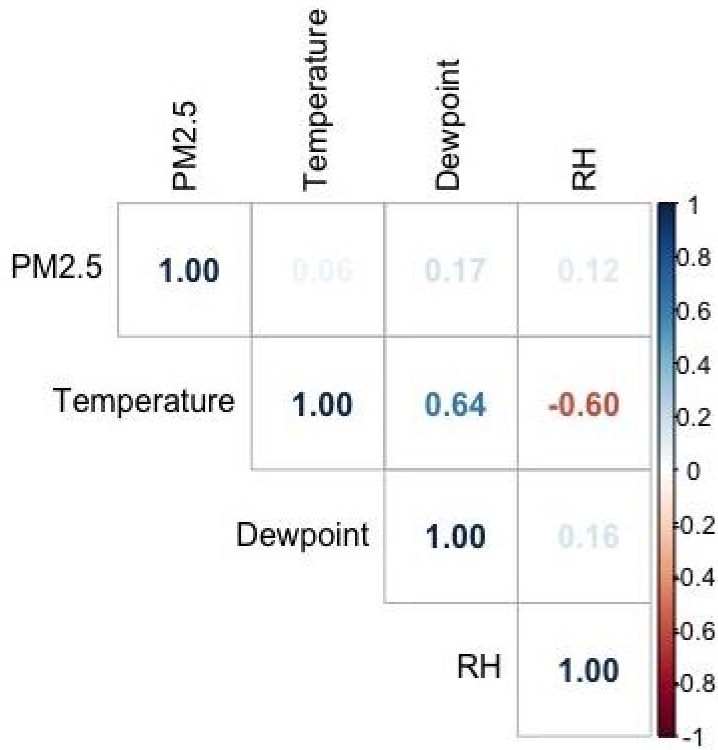


***Figure S8**: Correlations between $PM_{2.5}$, temperature, humidity and dewpoint for co-located LCS*

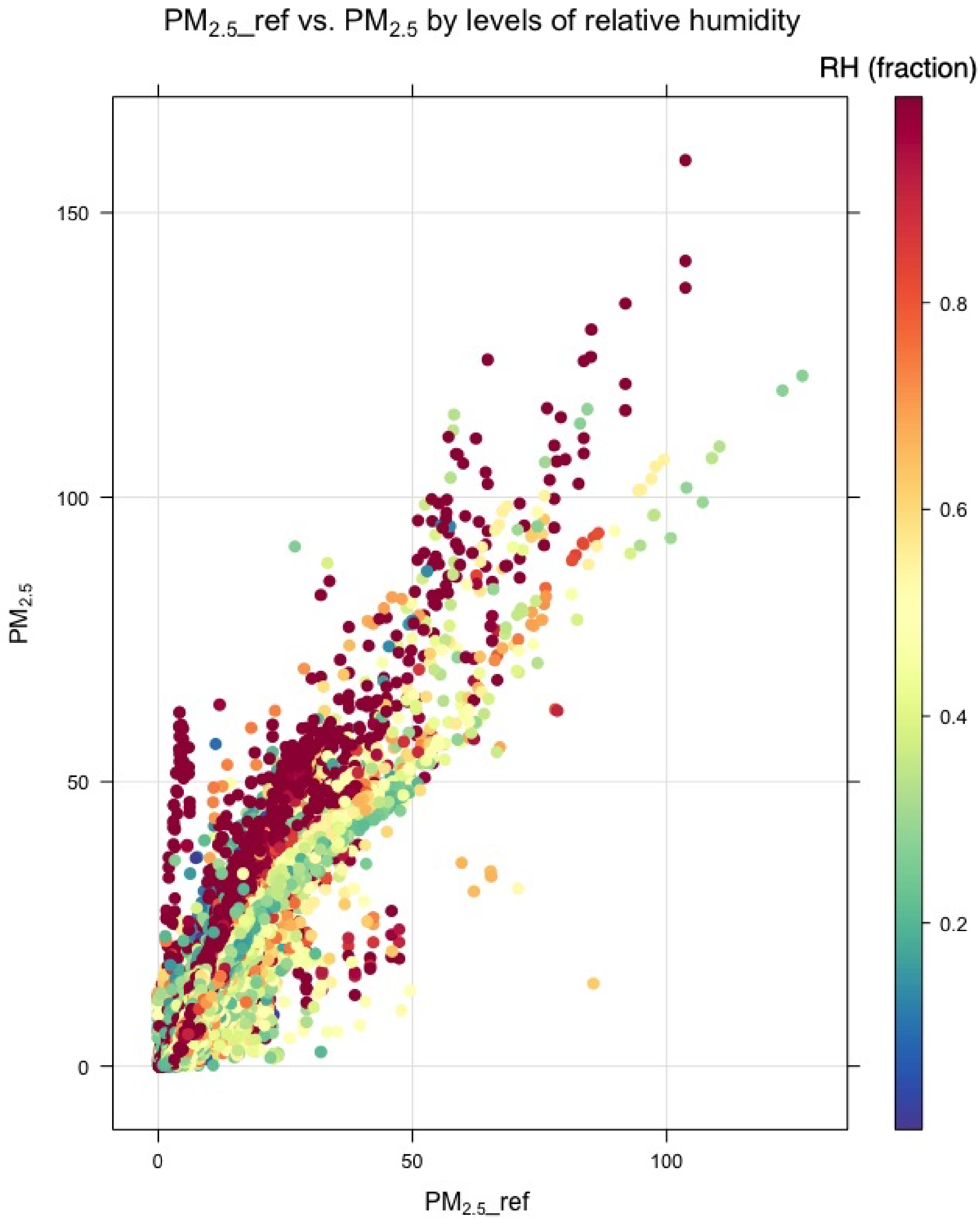


***Figure S9:*** *Comparison of hourly averaged PM$_{2.5}$ concentrations from reference monitors with the corresponding PM$_{2.5}$ concentrations from all co-located Love My Air sensors by levels of RH (expressed as a fraction)*

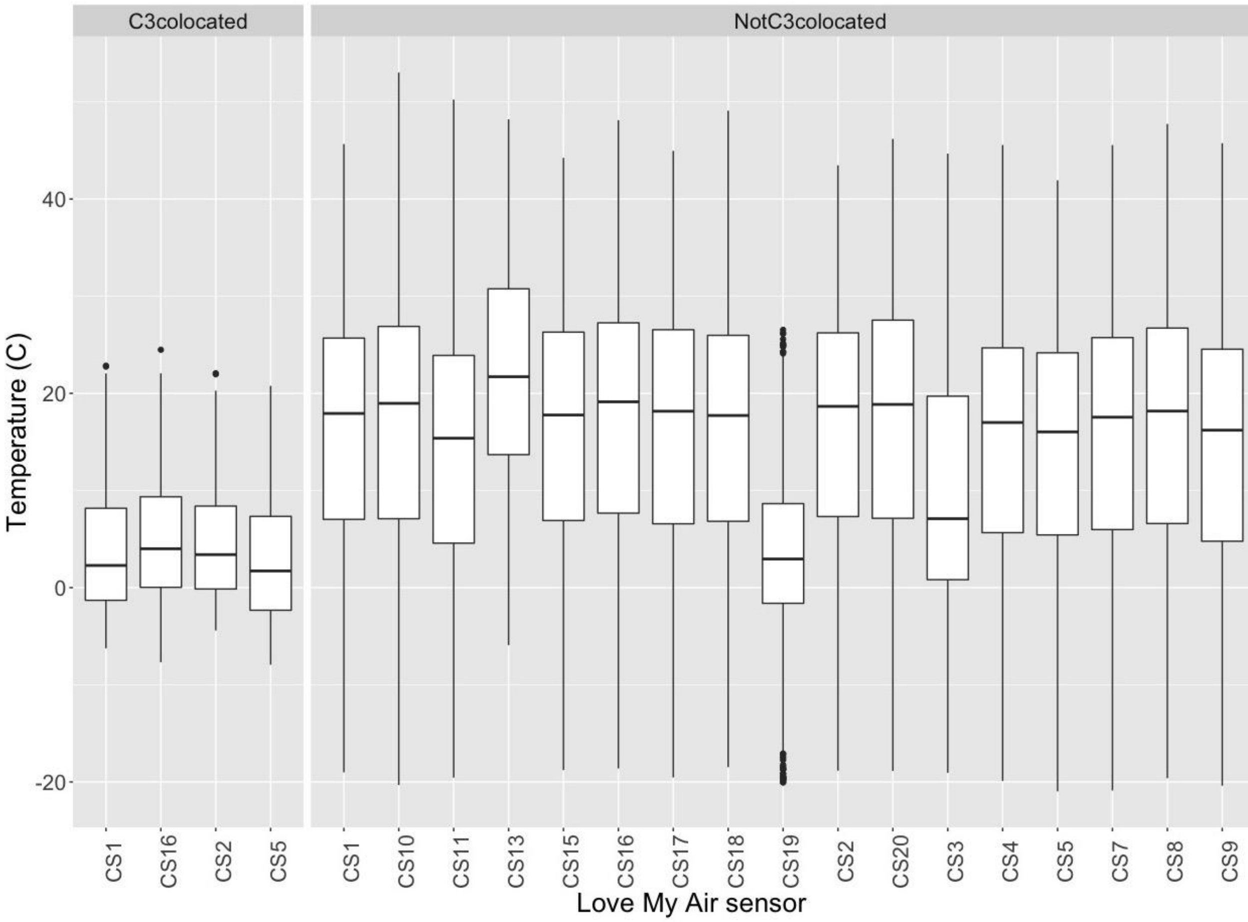


***Figure S10****: Distribution of temperature recorded by each Love My Air sensor. The distribution of temperature recorded by co-located LCS used in the C3 correction (Jan 1 - Jan 14, 2021 ) is shown on the left. The distribution of temperature recorded by all LCS not used to construct the calibration models are displayed on the right*

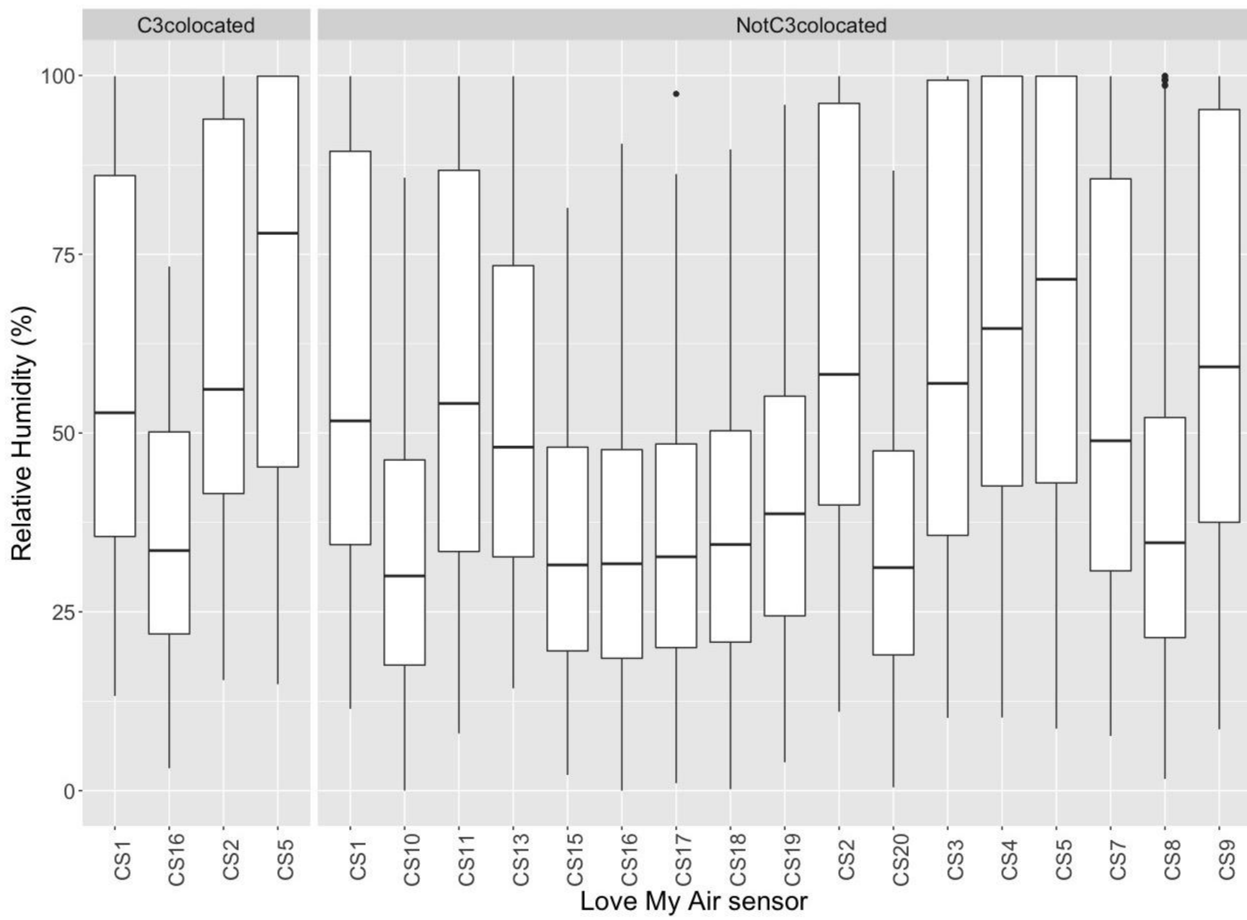


***Figure S11**: Distribution of RH recorded by each Love My Air sensor. The distribution of RH recorded by co-located LCS used in the C3 correction (Jan 1 - Jan 14, 2021 ) is shown on the left. The distribution of tRH recorded by all LCS not used to construct the calibration models are displayed on the right*

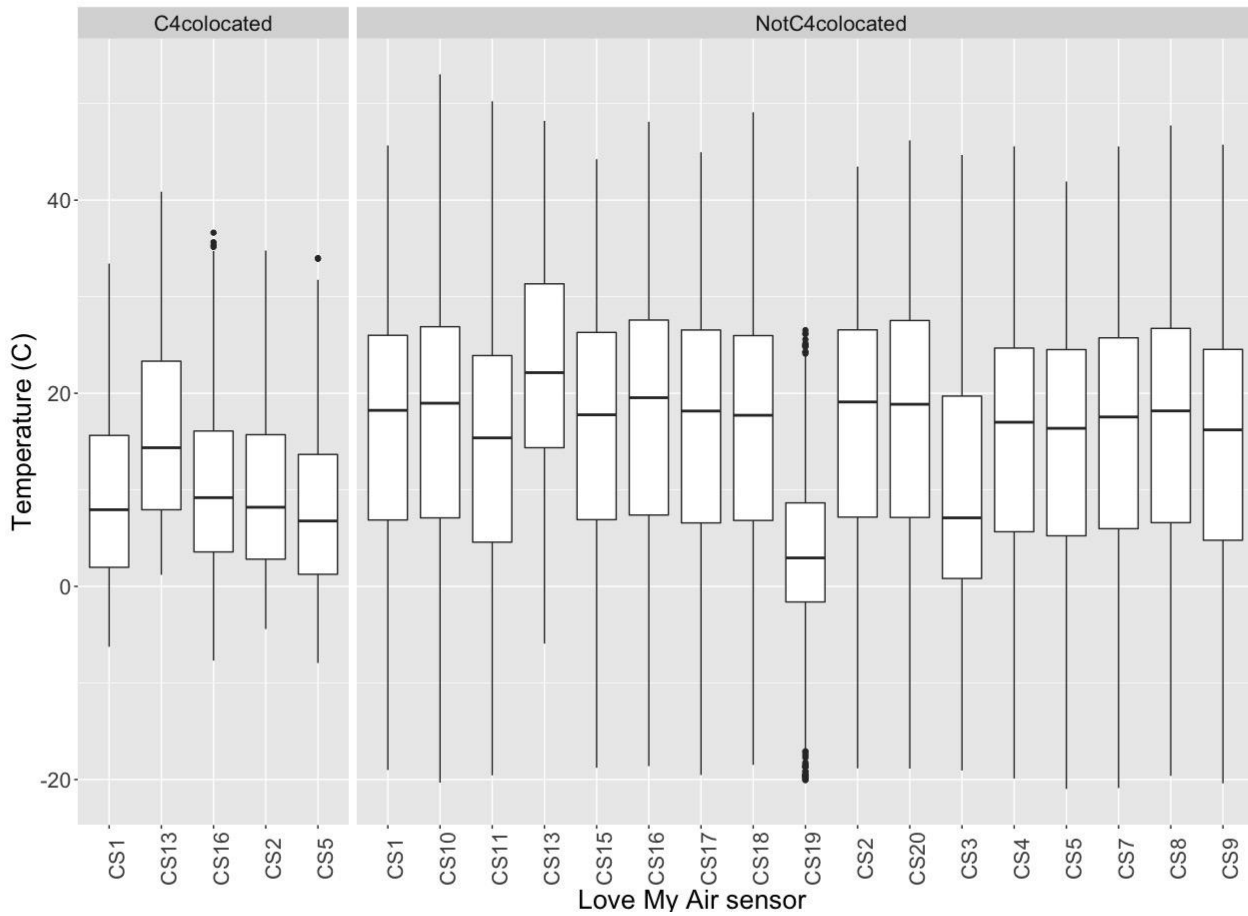


***Figure S12***: *Distribution of temperature recorded by each Love My Air sensor. The distribution of temperature recorded by co-located LCS used in the C4 correction (Jan 1 - Jan 14, 2021 and May 1 - May 14, 2021) is shown on the left. The distribution of temperature recorded by all LCS not used to construct the calibration models are displayed on the right*

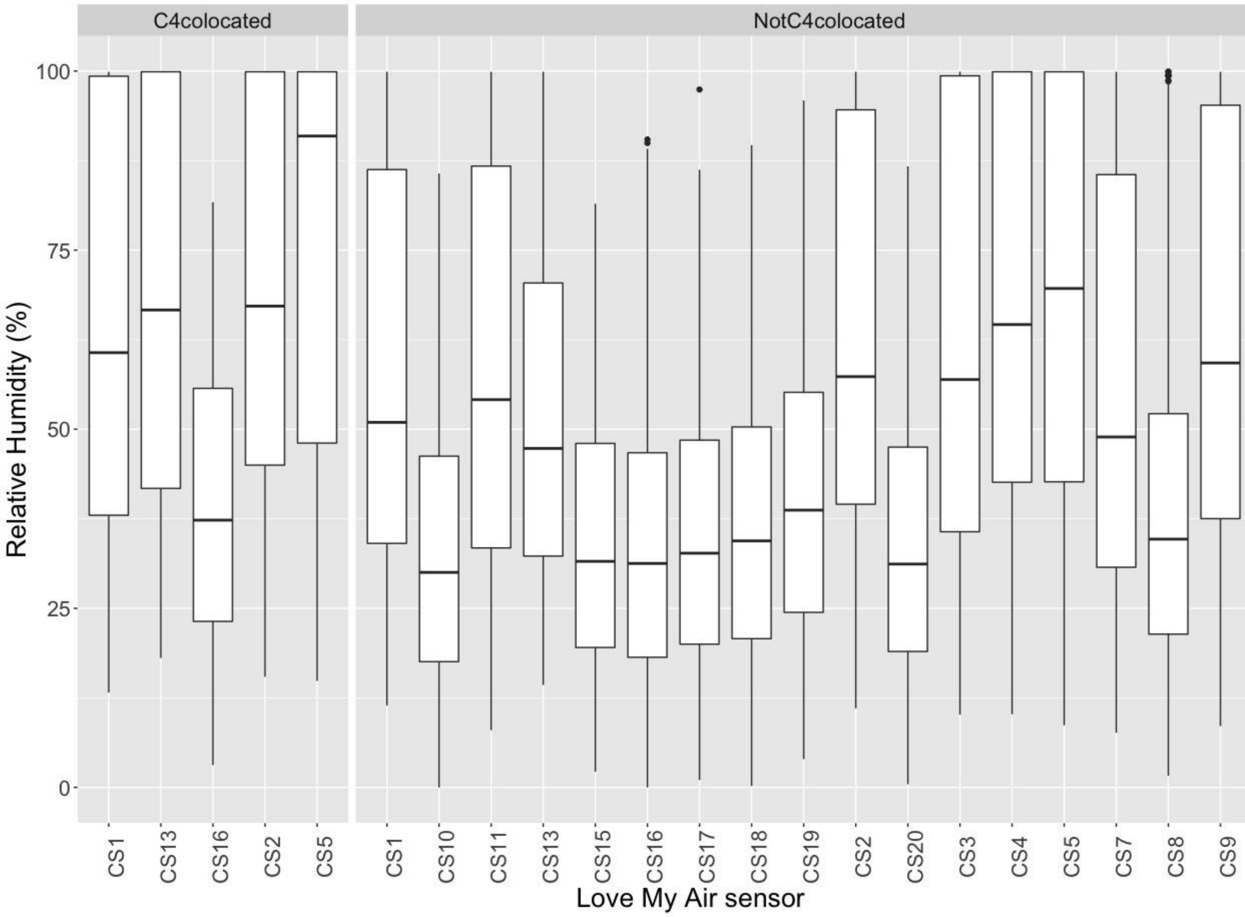


***Figure S13****: Distribution of RH recorded by each Love My Air sensor. The distribution of RH recorded by co-located LCS used in the C4 correction (Jan 1 - Jan 14, 2021 and May 1- May 14, 2021 ) is shown on the left. The distribution of tRH recorded by all LCS not used to construct the calibration models are displayed on the right*

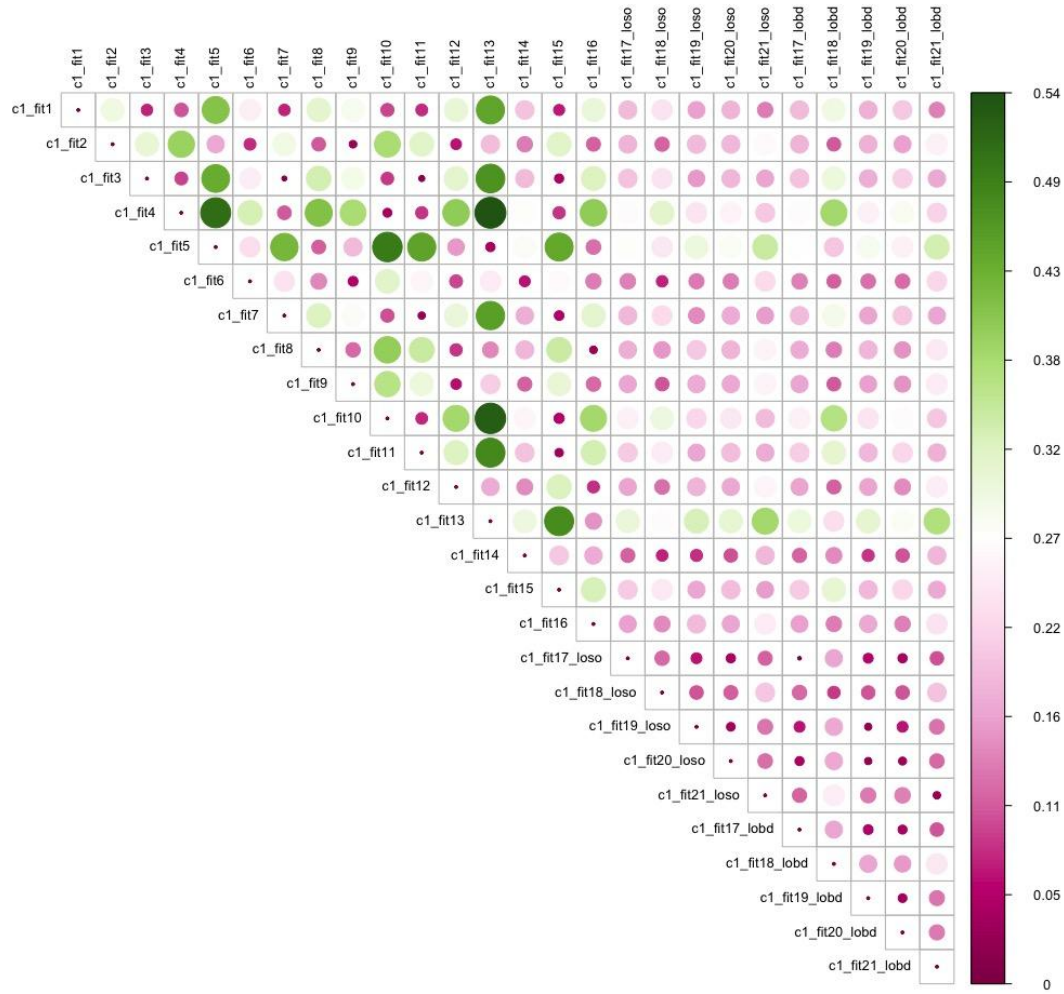


***Figure S14***: *Spatial RMSD* (µg/m$^3$) *from applying each of the 89 equations using correction C1 to all monitoring sites in the Love My Air network calculated using the method described in section 2.3.8*

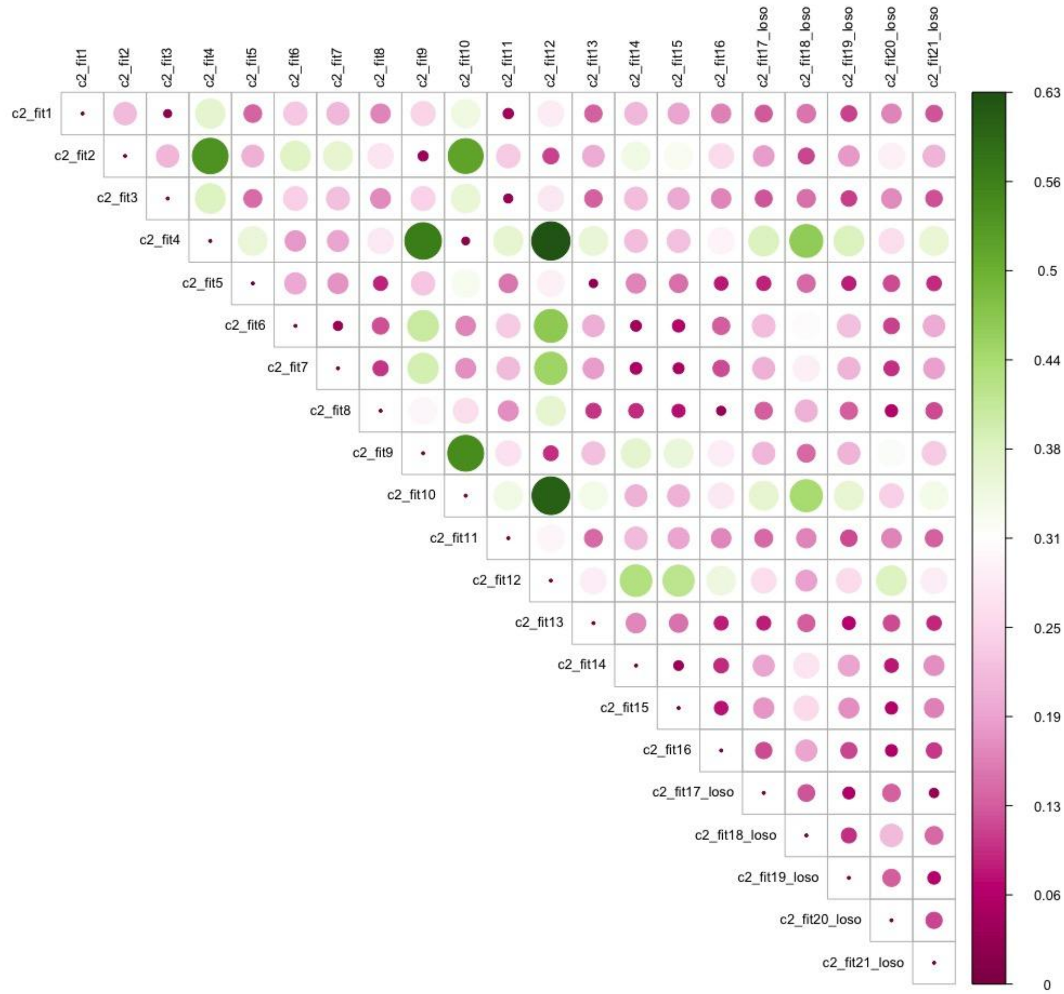


***Figure S15**: Spatial RMSD* (μg/m$^3$) *from applying each of the 89 equations using correction C2 to all monitoring sites in the Love My Air network calculated using the method described in section 2.3.8*

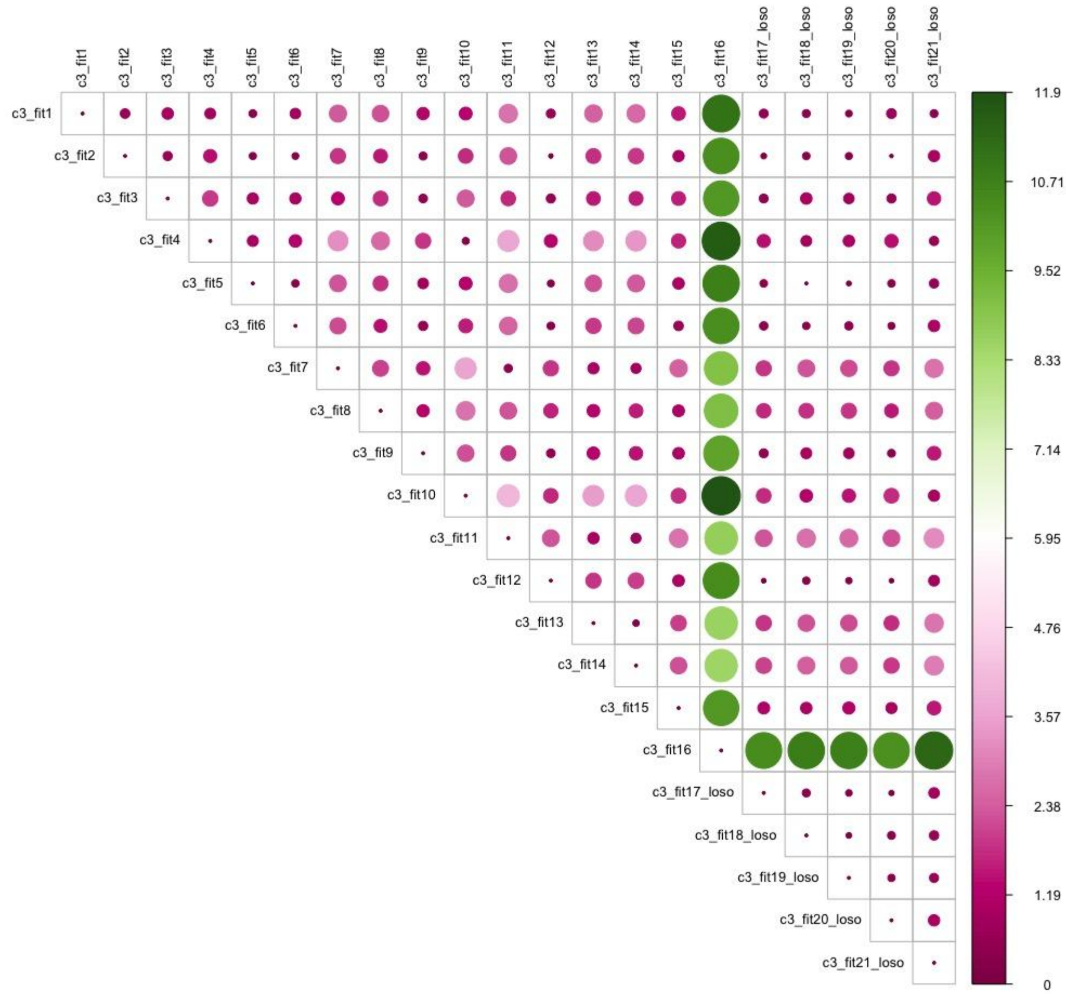


***Figure S16***: *Spatial RMSD* (μg/m$^3$) *from applying each of the 89 equations using correction C3 to all monitoring sites in the Love My Air network calculated using the method described in section 2.3.8*

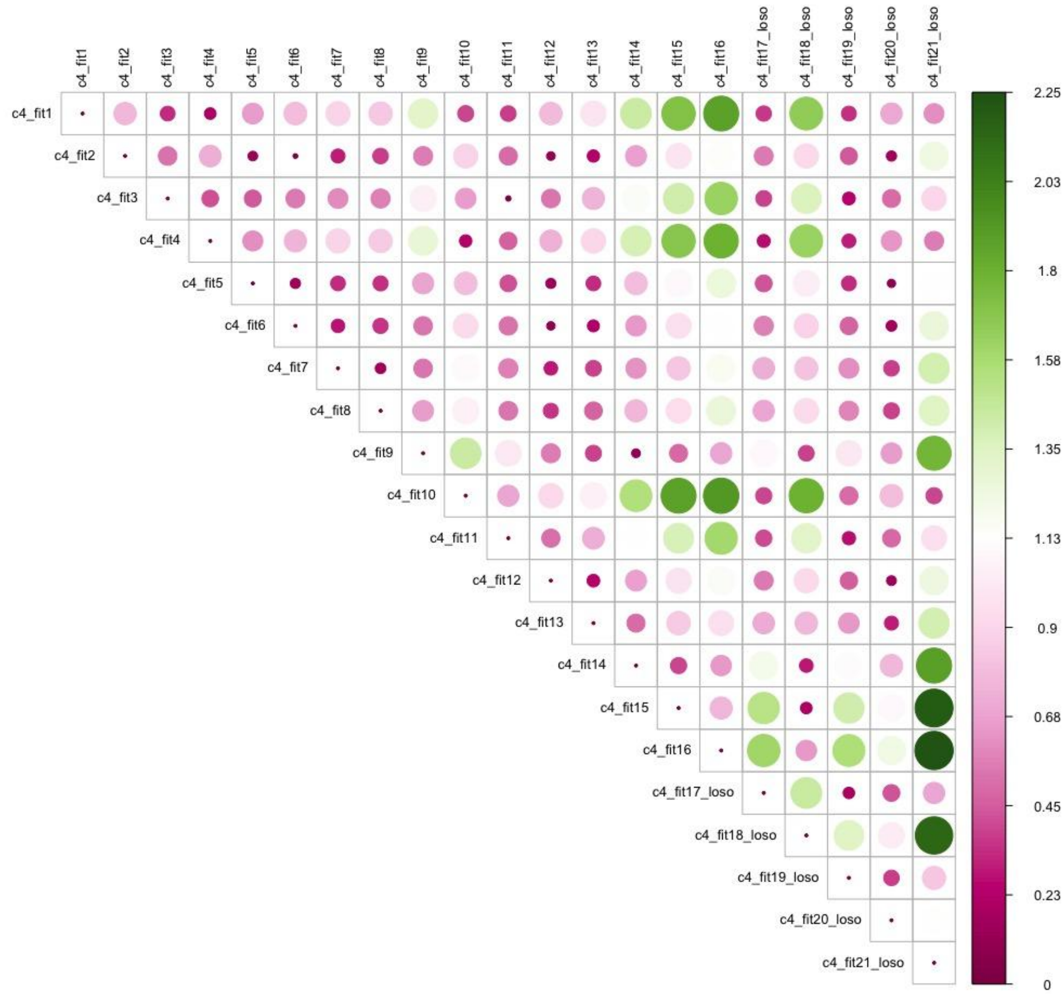


***Figure S17**: Spatial RMSD* (μg/m$^3$) *from applying each of the 89 equations using correction C4 to all monitoring sites in the Love My Air network calculated using the method described in section 2.3.8*

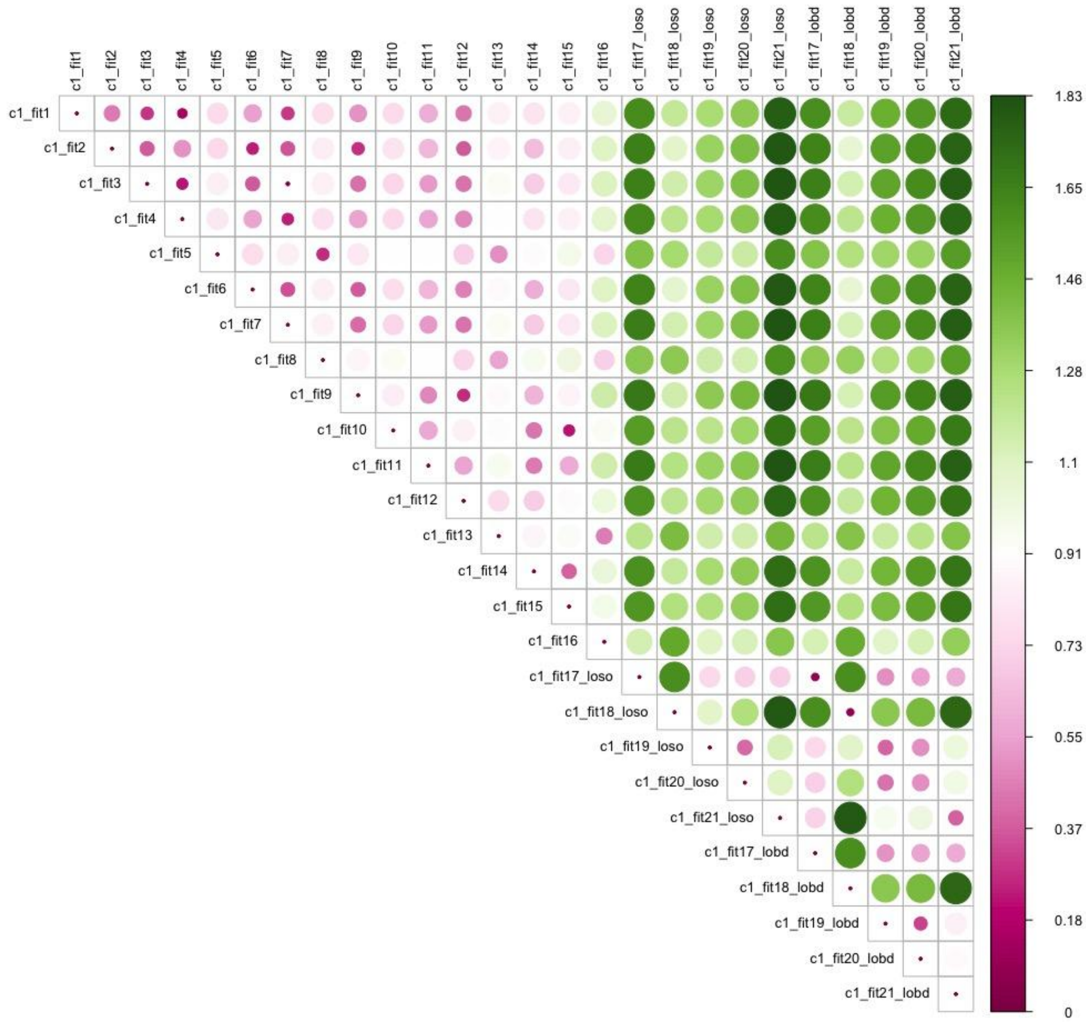


***Figure S18**: Temporal RMSD* (μg/m$^3$) *from applying each of the 89 equations using correction C1 to all monitoring sites in the Love My Air network calculated using the method described in section 2.3.8*

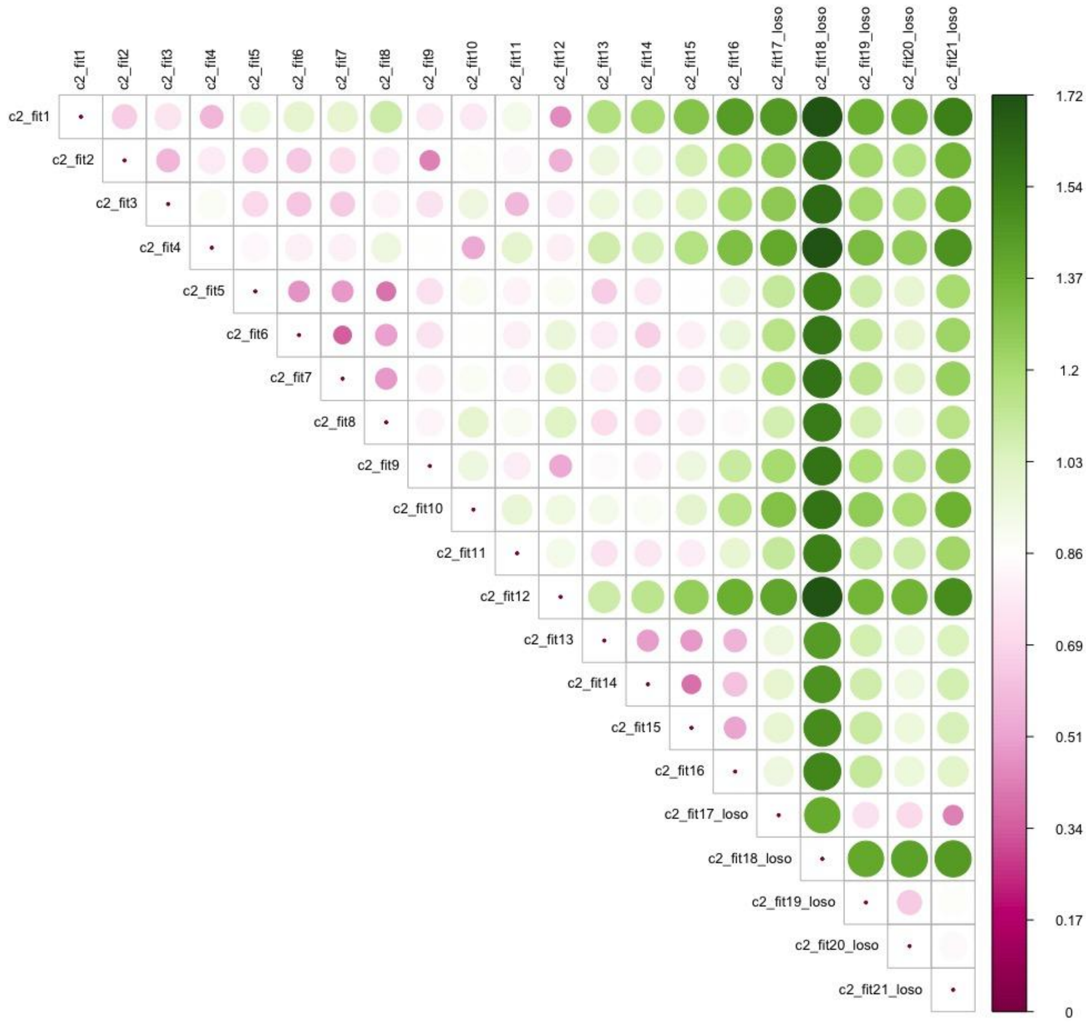


***Figure S19****: Temporal RMSD* (µg/m$^3$) *from applying each of the 89 equations using correction C2 to all monitoring sites in the Love My Air network calculated using the method described in section 2.3.8*

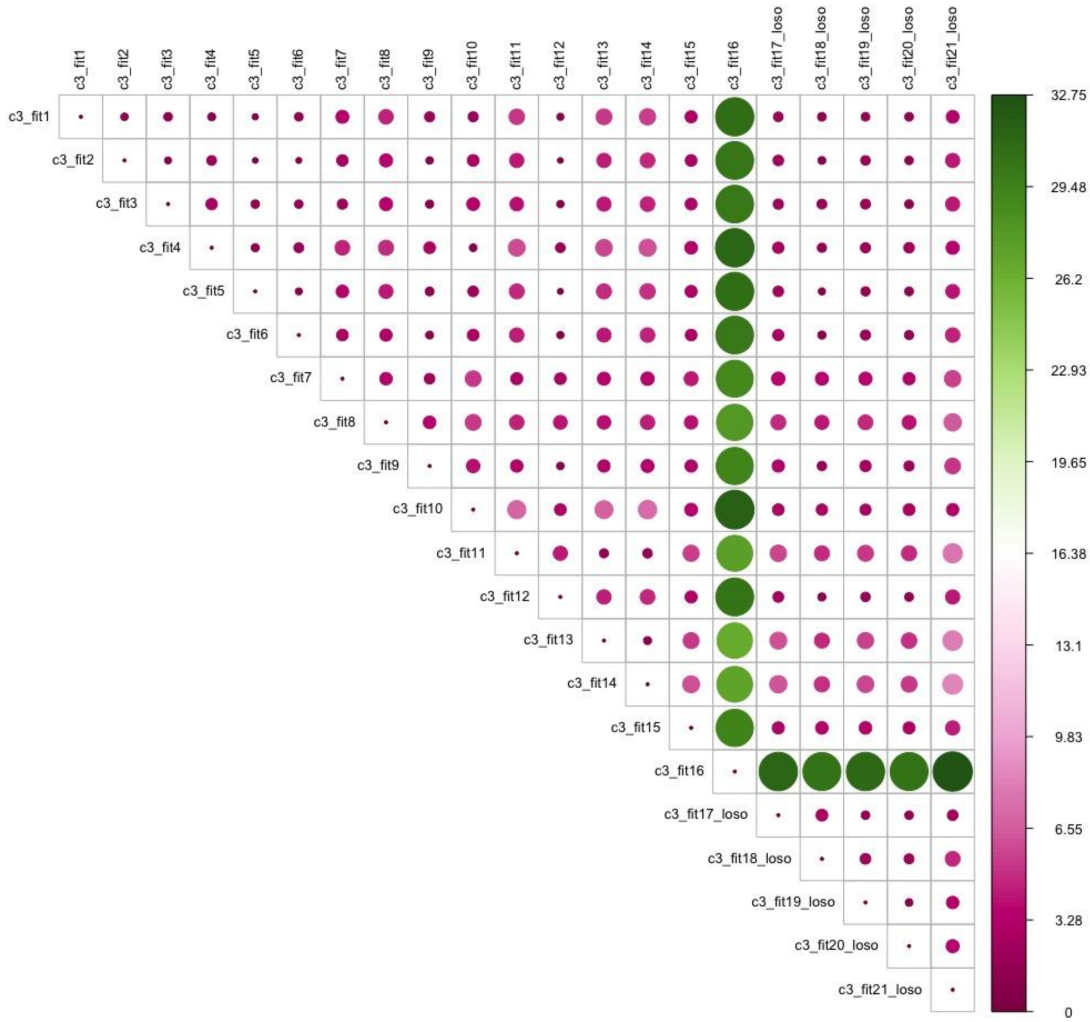


***Figure S20**: Temporal RMSD* (µg/m$^3$) *from applying each of the 89 equations using correction C3 to all monitoring sites in the Love My Air network calculated using the method described in section 2.3.8*

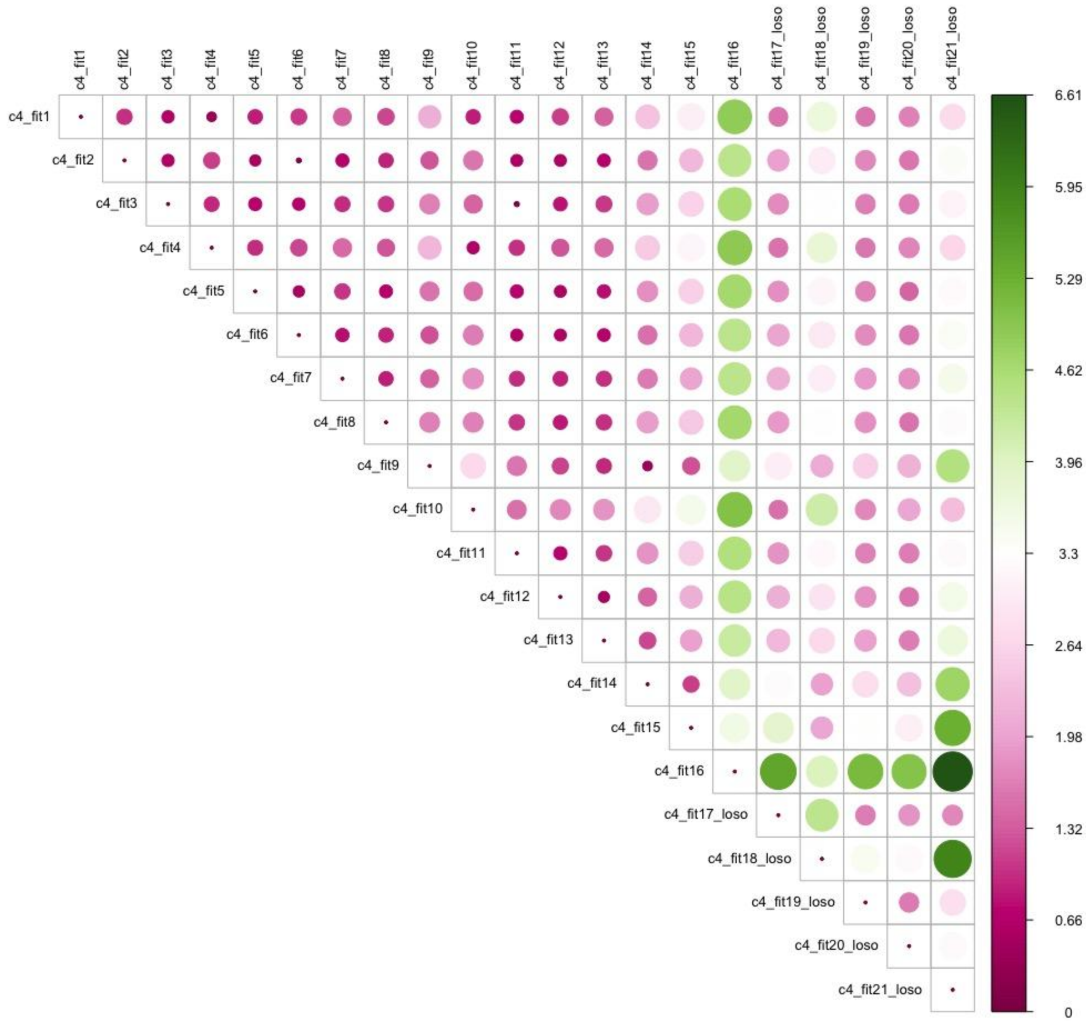


***Figure S21**: Temporal RMSD* (μg/m$^3$) *from applying each of the 89 equations using correction C4 to all monitoring sites in the Love My Air network calculated using the method described in section 2.3.8*

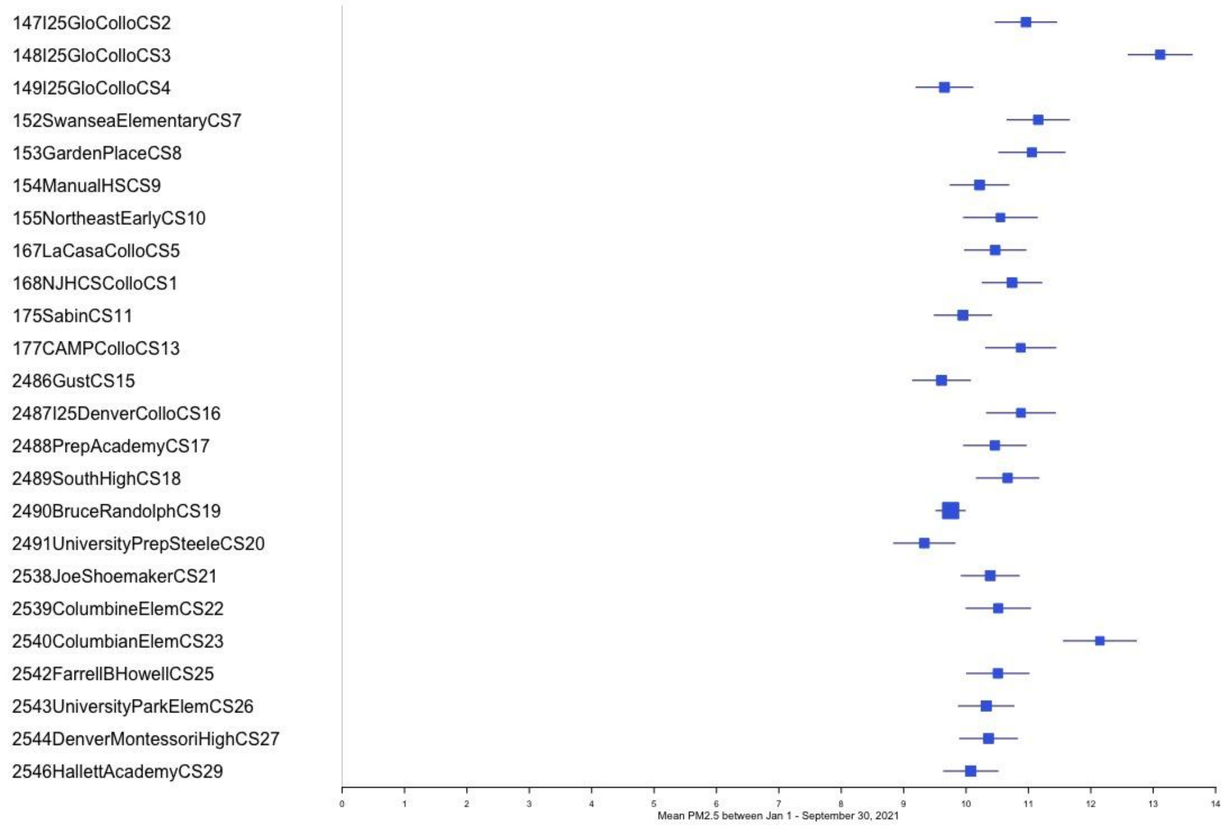


***Figure S22:*** *Mean (95% CI) $PM_{2.5}$ levels across the different models and corrections at each Love My Air site for the duration of the experiment (Jan 1 - September 30, 2021)*

# References

Johnson, N. E., Bonczak, B., and Kontokosta, C. E.: Using a gradient boosting model to improve the performance of low-cost aerosol monitors in a dense, heterogeneous urban environment, Atmospheric Environment, 184, 9–16, https://doi.org/10.1016/j.atmosenv.2018.04.019, 2018.

Spinelle, L., Gerboles, M., Villani, M. G., Aleixandre, M., and Bonavitacola, F.: Calibration of a cluster of low-cost sensors for the measurement of air pollution in ambient air, in: 2014 IEEE SENSORS, 2014 IEEE SENSORS, 21–24, https://doi.org/10.1109/ICSENS.2014.6984922, 2014.

Van der Laan, M. J., Polley, E. C., and Hubbard, A. E.: Super learner, Statistical applications in genetics and molecular biology, 6, 2007.

Zimmerman, N., Presto, A. A., Kumar, S. P. N., Gu, J., Hauryliuk, A., Robinson, E. S., Robinson, A. L., and R. Subramanian: A machine learning calibration model using random forests to improve sensor performance for lower-cost air quality monitoring, Atmospheric Measurement Techniques, 11, 291–313, https://doi.org/10.5194/amt-11-291-2018, 2018.

Zusman, M., Schumacher, C. S., Gassett, A. J., Spalt, E. W., Austin, E., Larson, T. V., Carvlin, G., Seto, E., Kaufman, J. D., and Sheppard, L.: Calibration of low-cost particulate matter sensors: Model development for a multi-city epidemiological study, Environment International, 134, 105329, https://doi.org/10.1016/j.envint.2019.105329, 2020.